Letters in Applied NanoBioScience
Open-Access Journal (ISSN: 2284-6808)

Review
Volume 12, Issue 1 2023, 6
https://doi.org/10.33263/LIANBS121.006

Critical Review on the Photodegradation Ability of Graphene and its Derivatives against Malachite Green, Methylene Blue, and Methyl Orange

Peetam Mandal [1], Jhuma Debbarma [1], Mitali Saha [1,*]

[1] Department of Chemistry, National Institute of Technology Agartala, Tripura – 799046, India
* Correspondence: mitalichem71@gmail.com (M.S.);

Scopus Author ID 55779373600

Received: 6.10.2021; Accepted: 15.11.2021; Published: 8.01.2022

Abstract: Owing to the oxidizing, catalytic ability, and adsorbing property, graphene-based composites and their derivatives have been an ideal component for water purification and thereof. The colossal poly-aromatic π–π network and oxygen-rich groups within the functionalized graphene materials play a decisive interaction with the water pollutants viz. agricultural run-off, industrial dye effluents, and bio-medical waste via electrostatic interactions, hydrogen bonding, and photon enriched oxidations. Among various pollutant dyes, malachite green (MG), methylene blue (MB), and methyl orange (MO) have been used extensively by aqua cultural farms, tanneries, research fraternities, and textile industries due to their multifarious usage. This review unveils the cost-effective graphene preparation from various chemical synthesis processes over other conventional methods and its effectiveness in removing MG, MB, and MO with composites comprising carbonaceous materials, metal oxides, metal hybrids, and conducting organic polymers. The adsorption capacities, pseudo-1st order kinetics, degradation efficiency, and pH had been highlighted chronologically to draw a conclusive nature of graphene and its derivatives as a potential remedial against these three pollutant dyes. This article also focused on various emerging materials that had been used with functionalized graphene recently to enhance degradation efficiency and expunge multiple toxic dyes for advanced water treatment processes.

Keywords: graphene oxide; malachite green; methylene blue; methyl orange; photodegradation; adsorbent; photocatalysis; graphene; pollutant dyes; degradation efficiency.

© 2022 by the authors. This article is an open-access article distributed under the terms and conditions of the Creative Commons Attribution (CC BY) license (https://creativecommons.org/licenses/by/4.0/).

1. Introduction

In contrast to other allotropes of carbon, graphene has its significance with extraordinary chemical and physical properties making its application highly diverse than other allotropes, i.e., diamond, graphite, or CNT. Earlier mono-layered graphene has found its usage in electronics and solar cells, while bi-layer, tri-layer, and few layers had shown remarkable properties in contrast to single-layer graphene. Recently, the chemical and physical properties of multi-layered graphene highlighted its application in catalysis as well as an eco-friendly adsorbent in the environmental cause, but the preparation of graphene has been quite subtle and challenging ever since its discovery. Commercially, graphene was prepared from graphite precursors. A high-quality mono-layer is derived from sophisticated chemical vapor deposition (CVD), laser ablation, and plasma arc processes, making the finished product highly expensive. However, environmental crisis and decontamination of toxic effluents require functionalized graphene derivatives.

Away from this production monopoly - relying vastly on graphite precursor and exfoliation technique, the solubility of graphene hindered in various chemical reactions as traditional knowledge portrays pristine graphene doesn't disperse or blend in any solvent. The functionalization of graphene with various functional groups and hetero atoms had solved the dispersion issue in solvents and aqueous medium, relying completely on the conventional Hummers method and improved Hummers method [1, 2]. Therefore, substantial efforts were made to create graphene, a multi-dimensional research-operating, and industry-friendly material, to perfect its dispersion in various solvents, including an aqueous medium at a much-reduced cost. Fortunately, the preparation from non-graphitic sources over the last few years has been a steady trend amongst industries and research fraternities to address this dispersion issue. Thus, apart from CVD, bottom-up synthesis from organic molecules in the solid and liquid phase has emerged but is still in its genesis stage with niche applications.

Apart from dispersion in solvents, the bottom-up strategy had been quite impeccable for inserting hetero-atoms at the desired positions within the graphitic sheet and designing the length, breadth, and chain of graphene derivatives. The absence of a governing principle and fundamental chemistry behind the formation of graphene and its derivatives from organic monomers made this entire synthesis quite challenging. Economical production of scalable graphene and its derivatives is the success mantra, but the ability to combat environmental issues will be a vital advantage. Amongst various inorganic and organic pollutants discharged into the water body, the organic effluents, including organo-phosphorus, detergents, organo-chlorine, petroleum, aromatic compounds, polymers, and dyes, had been the most detrimental for living organisms.

The complex aromatic structure of dyes makes them highly soluble in an aqueous system and difficult to bio-degrade in the discharged water bodies from various industries. Synthetic dyes like malachite green (MG), methylene blue (MB), and methyl orange (MO) are mandatory to be treated before discharging as effluents within permissible limits as prescribed by environmental regulations. These are highly resistant to light and mild oxidizers, but complete removal by basic anaerobic digestion isn't possible. However, treating these colored effluents with a single conventional method such as like ozonation, coagulation, membrane filtration, or flotation would decolorize partly, and therefore photodegradation is an attractive alternative. In this article, an extensive literature survey revealed functionalized graphene against three commonly used pollutant dyes, i.e., MG, MB, and MO were done.

2. Synthesis of Graphene and its Derivatives from Chemical Methods

In contrast to 'top-down' approaches involving shear exfoliation and abrasive wear [3, 4], 'bottom-up' synthesis enables control on the graphene sheet structure due to judicious designing of monomer molecule through polymerization/ aromatization or graphitization. At specific positions, this bottom-up chemical synthesis strategy enables precise doping, making graphene functional with heteroatoms very definite. The earliest chemical synthesis was chemical vapor deposition (CVD) which was attributed to the synthesis of carbon-nanotube (CNT) and had been well dominated in the chemical assembly of molecules to prepare graphene ever since its discovery. Similarly, graphene preparation from non-graphitic precursors was done using epitaxial growth from SiC precursors in the vapor phase. Other methods like plasma arc discharge and laser induction process relied on non-graphitic precursors. Still, the sophisticated instruments and inert conditions make these methods dependent on gaseous phase akin to CVD. According to Web of Science, the histogram

portrayed in Figure 1, revealed the increase in CVD usage for graphene preparation over other preparation techniques chronologically.

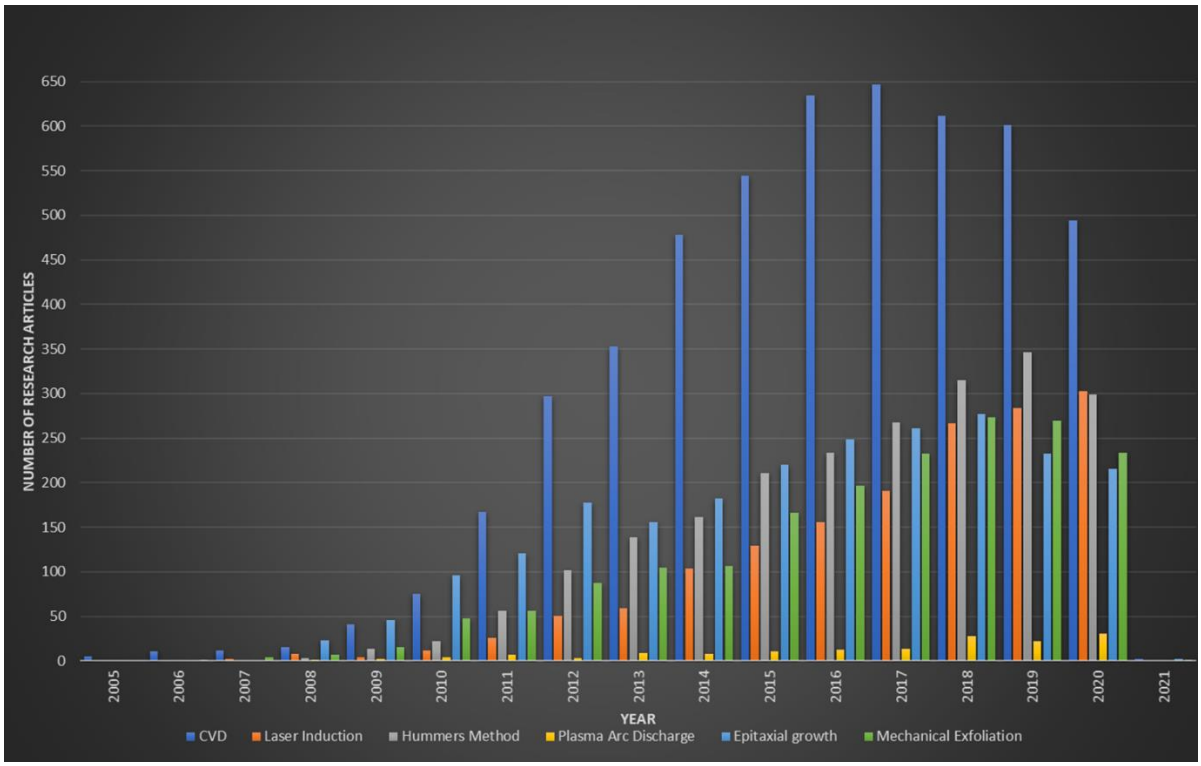

Figure 1. Total number of articles with different preparation methods for graphene and its derivatives.

Thus, designing the graphene sheet with controlled features relies on non-graphitic precursors rather than natural graphite. A literature survey shows over 5000+ research articles only on the usage of CVD to design graphene derivatives on various substrates. However, the economic aspect and energy sustainability are hampered with CVD due to high temperature, sophisticated set-up, inert atmosphere, and gaseous phase, making the cost reliability of graphene beyond the scope of commercialization. Synthesis of graphene and its derivatives via condensation and aromatization of organic molecules in solid-phase via heat treatment had been a new strategy as well as economically feasible. Hence, to avoid the vapor phase and continue synthesis in solid-phase heat treatment from non-graphitic precursors, Dong *et al*. first reported the synthesis of GO from citric acid [5]. Initially, GQD was prepared, and after prolonged heating GO was formed at 200^{o} C on prolonged heating; however, the fundamental mechanism behind this synthesis route was uncleared.

Awe-inspiringly, various coupling reactions including Suzuki, Heck, Negishi, Sonogashira, and Ullmann reaction had been a part of graphene synthesis with the concept of coupling of large aryl halide molecules into graphitic sheet via condensation and polymerization. In 2008, Yang *et al*. synthesized armchair graphene nanoribbons based on Suzuki-Miyaura polymerization from diiodobenzene using $FeCl_3$ catalyst [6]. This particular Suzuki-Miyaura coupling was also observed in the polymerization of 1,2-dibrombobenzene using Pd catalyst into armchair graphene ribbons with a poor yield ~ 56% [7]. This coupling was also performed by Li *et al*. to obtain a graphene armchair under an inert atmosphere using $Pd(P^tBu_3)_2$ catalyst with a 73% yield [8]. On the principle of Yamamoto polymerization, Gemayel and co-workers prepared nanoribbons of graphene from dichloride condensation followed by oxidative addition using Ni catalyst [9]. Similarly, Huang *et al*. synthesized para-armchair graphene nanoribbons with bulky side chains via Yamamoto coupling followed by Diels-Alder reaction of anthracenyl groups [10].

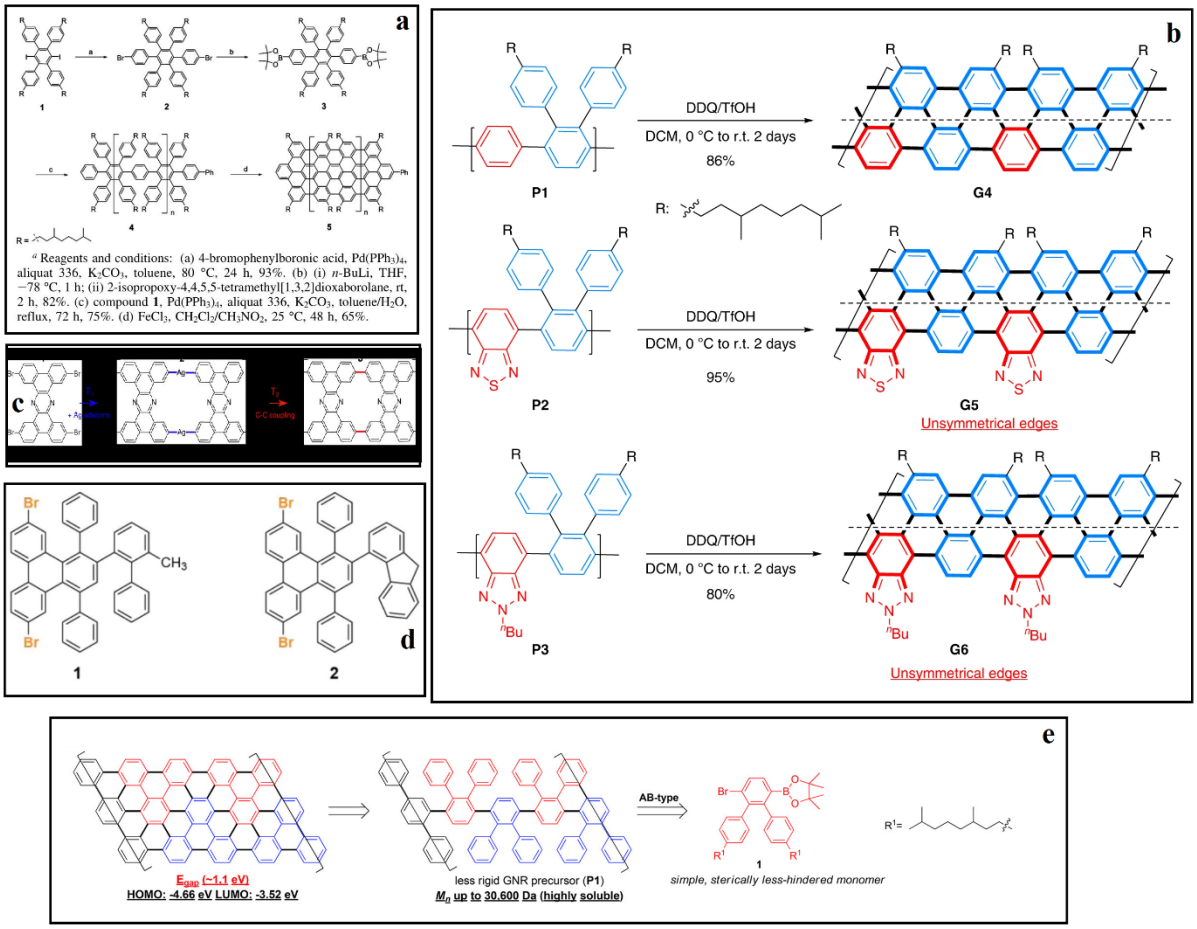

Figure 2. Schematics of the formation of graphene products from various precursors via chemical synthesis; **(a)** Synthesis of graphene nanoribbons [6]. Reprinted with permission from ref [6]. Copyright 2008 American Chemical Society; **(b)** Synthesis of graphene nanoribbons. Syntheses of N = 6 aGNR and its edge-functionalized analogs [8]. Reprinted from open-source ref [8]; **(c)** Hierarchical Ullmann coupling for the generation of porous N-doped Graphene Nanoribbons [11]. Reprinted with permission from ref [11]. Copyright 2020 American Chemical Society; **(d)** Schematic representation of molecular precursors 1 and 2 used to prepare chevron-type nanoporous graphene [12]. Reprinted with permission from ref [12]. Copyright 2020 American Chemical Society; **(e)** Bottom-up solution synthesis of N=9 armchair graphene nanoribbons [7]. Reprinted with permission from ref [7]. Copyright 2016 John Wiley & Sons.

Notably, nanoribbons of graphene with 50 nm length were designed from poly(p-phenylene ethynylene) molecule instead of conventional small halide monomer utilizing Sonogashira coupling, relying on CuI catalyst [13]. In 2020, Jacobse and co-workers recently fabricated nano-porous graphene on Au substrate under a nitrogen atmosphere [12]. In figure 2, various precursors were represented to synthesize graphene and its derivatives via different couling reactions chemically. In a similar fashion, N-doped graphene nanoribbons were constructed using silver catalyzed Ullmann polymerization [11]. Henceforth, it can be clearly understood that coupling reactions followed by polymerization were suitable for designing graphene nanoribbons with specific catalysts under specific reaction conditions and parameters; however, the yield of the product had been less than the conventional heat treatment method. On the other hand, heating organic molecules at their respective melting range in the solid phase were extremely limited and challenging. Concurrent to the existing polymerization of haloaryls, it was also found certain compounds like tartaric acid, m-aminophenol, citric acid, galactose, and glucose effectively produced functionalized graphene in a single step [14, 15].

3. Photocatalytic Degradation of Dyes with Functionalized Graphene and its Derivatives

The extensive wastewater disposal into waterbodies from industries containing organic dyes led to fatal jeopardy for human and aquatic life ubiquitously. The global production of these organic dyes releases 5 – 20% of the dyes as textile effluents into the ecosystem [16]. The remedy against such critical water pollution issues had been hydrolysis, oxidation of these dyes, and chemical reactions within the wastewater-using microorganism to create metabolites. Apart from these conventional treatments, the emergence of photocatalysts and their potential in decriminalizing toxic dyes has dwindled this problem meticulously. The photocatalytic efficiency of various materials to dissociate dyes decreases significantly due to the high recombination ratio of electrons and holes produced from irradiation of ultraviolet light. To compensate for this shortage, materials are exposed to prolong visible light sources making the process cost-effective. Moreover, there are various setbacks with powder-based catalysts like separation after every run and continuous stirring. The sedimentation process, filtration, and centrifugation are commonly used to recover spent catalyst, but a large portion of materials had been lost during the treatment of dyes.

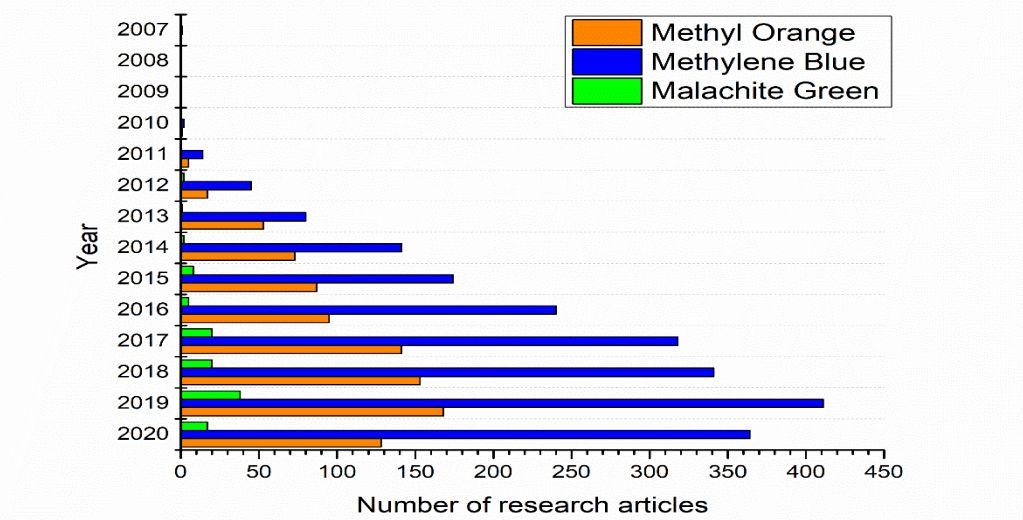

Figure 3. Total number of research articles with nanocomposites of graphene and its derivatives with metal nanoparticles in degradation of MG, MB, and MO.

Initially, metallic nanoparticles were largely used as photocatalysts, and currently, the trend has moved to demonstrate the synergistic effect of metal nanoparticles with ceramics, alloys, other metal nanoparticles, carbonaceous nanomaterials, and pyrolyzed products. Graphene and its derivatives have been used extensively with metal nanoparticles as nanocomposites and nano-hybrids to enhance the photo-catalytic ability. The high surface area of graphene-based materials promotes a high reactive site for these metal nanoparticles, but graphene acting solely as a photocatalyst is quite limited. Moreover, after prolonged use, their metallic counterparts tend to cause heavy metal pollution in water bodies and hamper soil quality [17]. The use of graphene and its derivatives solely as a photocatalyst is quite limited, and degrading major toxic dyes like malachite green, methylene blue, and methyl orange has been quite challenging. However, according to Web of Science, a literature report showed graphene's role with metal nanoparticles in decolorization of these three dyes had been severely used under the illumination of the ultraviolet and visible lamp. In figure 3, the histogram as per the Web of Science literature survey had shown the enormous figures of the use of graphene and its derivatives with metal nanoparticles in photodegradation of these three dyes. The exhaustive use of graphene with metal nanoparticles as nano-hybrid and nanocomposites

makes the material and process quite expensive apart from imposing the threat of metal toxicity in water.

Metals (viz. Cu, Ag, Au, Ni, Pd, Pt, Ti, Zr, Sn, Zn, Cd, Fe, Mn, Mo, Co, Y, W) had been used with graphene and its derivatives; hence metal toxicity is quite pronounced in search for a remedy against organic dye effluents. The complete literature survey of the use of only graphene and its derivatives in photocatalytic degradation of malachite green, methylene blue, and methyl orange has been shown in the forthcoming sections.

4. Photocatalytic Degradation of Malachite Green (MG) with Graphene and its Derivatives

The early use of malachite green was to control saprolegniasis in the aquaculture industry; since then, the annual production of malachite green has increased [18]. Nowadays, as a cationic dye, it has found its usage in food and medicine production also largely as a dye in biological staining, sericulture, paper, wood, tannery, and textile industries [19, 20]. Clinical investigation elucidated malachite green's hazardous and carcinogenic effects as a liver tumor promoter. The mammalian cells are susceptible to the high cytotoxic effects of malachite green, and humans suffer from respiratory tract irritation upon inhalation, and ingestion leads to gastrointestinal tract infections. Several cases had been reported about irritation to skin upon contact and permanent damage to the cornea. Thus, the detrimental effects on aquatic life mostly affect gonads, nephrons, gills, liver, and gonadotropic cells [21].

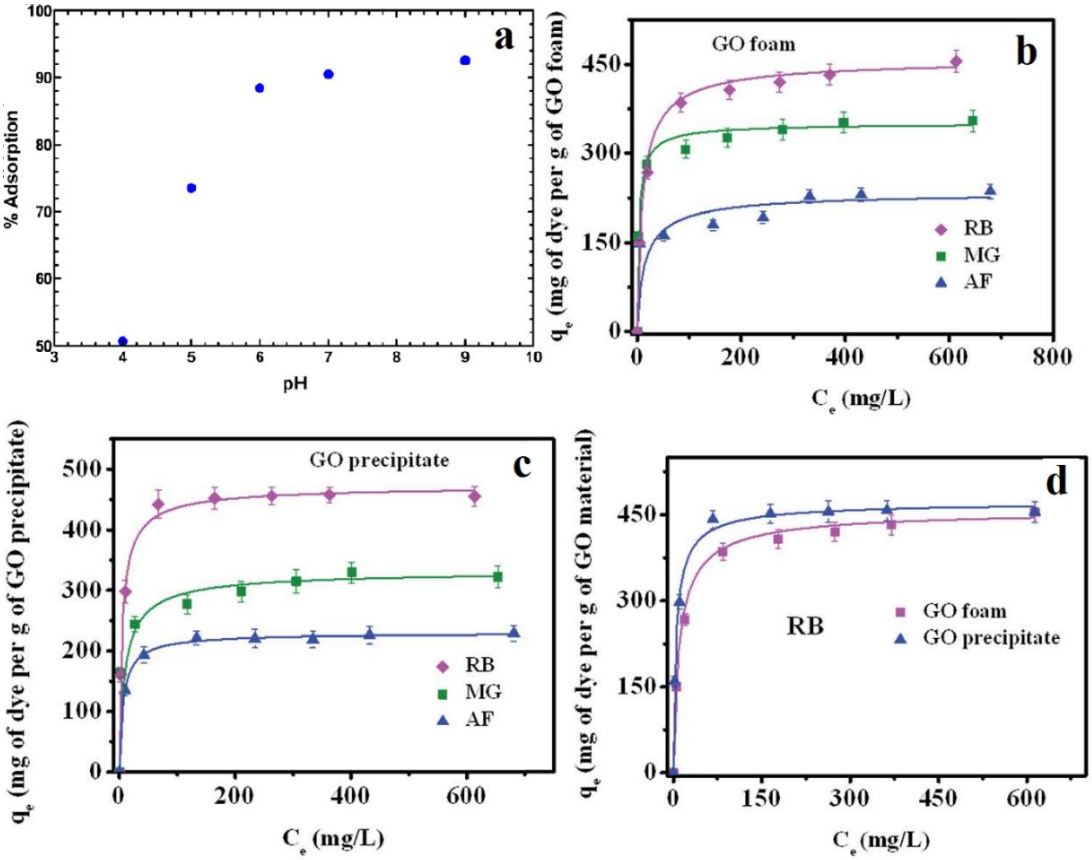

Figure 4.

Effect of pH in degradation of MG **(a)** Removal efficiency of methyl green onto GO nanosheets at different pH values and a temperature of 18 °C [22]. Reprinted with permission from ref [22]. Copyright 2012 American Chemical Society; Adsorption isotherms and the corresponding fitting plots of RB, MG and AF dye molecules on (b) GO foam, and (c) GO precipitate at 37 ºC and natural pH (~3). The concentration of GO foam is 0.3 g L^{-1}, and adsorption time is 8 h. (d) Comparison plot of adsorption isotherms of RB dye on GO foam and GO precipitate [26]. (b-d) Reprinted from open-source ref [26].

Sharma and Das, in 2013, reported the photodegradation of malachite green (MG) using graphene oxide (GO) prepared from the Hummers' method [22]. The dye sample was decolorized within 2 h, but the concentration was very low ≤ 10 ppm made the initiative approach quite feeble. Interestingly, the adsorption capacity increased with a gradual rise in pH towards alkalinity, as demonstrated in figure 4.a. A couple of years later, Zhang *et al*. reported the degradation of MG using graphene oxide caged within cellulose beads [23]. Varying the amount of GO, the decontamination was monitored, and >96 % of the dye content was removed after 24 h. Suresh and co-workers eliminated dual dye viz. MG and methylene blue with the advent of reduced graphene oxide (rGO) [24]. The material was reduced in a green process using cinnamon extract, but low concentrations of dyes ~ 5 ppm were degraded within 40 mins. Similarly, to sustain a green process, Upadhyay et al. synthesized rGO from grape extract and used it to remove MG [25]. Upon comparing GO and rGO, the latter exhibited complete degradation within 6 h while GO decolorized MG within 3 h.

In 2016, Rathour and co-workers obliterated 79 % of MG with GO nanosheets at pH 8, but the increase in the dye concentration led to the decline of degradation percentage [27]. Robati *et al*. used GO and rGO to decompose MG in various pH environments [28]. It was found at acid medium, the adsorption was significantly high for GO than rGO. At the same time, the temperature was elevated to 308 K. In a facile green process, 3D porous graphene hydrogel was synthesized by Shi et al. and was used in pseudo-first-order removal of 140 ppm MG, MB, and crystal violet [29]. The doping of nitrogen and sulfur in graphene hydrogen enhanced the degradation process due to electrostatic interactions and π-π interactions with the dye molecule. Although the photocatalytic reactions degraded the dye at high concentrations, the temperature and pH dependency factor cannot be underestimated for industrial scale. The immiscible nature of GO requires constant stirring; therefore, to avoid settling of the photocatalyst Jayanthi *et al*. synthesized GO foams to decolorize acriflavine, MG, and rhodamine B (RB) [26]. The 3D architecture of GO adsorbed MG in an alkaline medium, but the dye concentration was subsequently very low ~ 10 ppm (figure 4b-d). Gupta and Khatri used high surface area (~ 931 m^2 gm^{-1}) rGO to wane MG level in simulated waste water model [30]. Complete degradation was possible in acidic conditions (pH 3.7); however, the process was tedious ~ 7 h. In 2018, Wei *et al*. performed the detection of MG in fish extracts using GO nanosheets. The sensing detection was based on the spray-ionization substrate in mass spectrometric technique; however, 98% of MG was converted into leuco-malachite green metabolite [31]. Sykam *et al*. reduced GO using tulsi green tea, and the synthesized rGO was used in supercapacitors and degradation of 50 ppm MG, MB, and methyl orange (MO) [32]. At pH 6, the degradation of MG is quite pronounced, and the adsorption capacity of MG maximized to 416 mg gm^{-1}. A year later, Xing and co-workers fabricated GO and rGO from needle coke to decolorize 100 ppm MG solution [33]. The results highlighted that the multilayered graphitic planes of GO prepared from coke had high adsorption capacity than conventional GO prepared from natural graphite. Tang *et al*. prepared amphiphilic graphene-based aerogel to degrade multiple dyes viz. MG, MB, MO, and RB at various pH [34]. The material successfully adsorbed four hazardous dyes, but the dye concentration was low ~ 20 ppm, and the catalytic cycle of the photocatalyst didn't exceed over thrice. In 2020, Wang *et al*. functionalized GO with acrylic acid to degrade multiple dyes, i.e., MG, MB, MO, and RB [35]. The adsorption of MG was ~ 582 mg gm^{-1} with 100-ppm dye concentration; however, the pH was maintained at high alkaline conditions (pH ~ 10). The dispersive enhancement of GO further in an aqueous medium with aminated lignin was carried out by

Chen and co-workers, which was further used to remove MG from wastewater [36]. The results were promising with 91% decolorization, and it remained ~ 89 % after the 5th cycle. Söğüt *et al*. synthesized sulfonated rGO for Zn uptake, and degradation of MG was carried out under pH 9-10 [37]. The adsorptive capacity increased with the sulfur-based functionalized groups of GO, but the degradation was subjected to heat treatment ~ 80^{o} C. Recently, the Chinese research team degraded 100 ppm of MG, MB, MO, RB, and acid orange with acid orange sulfur-doped GO [38]. Interestingly, the degradation didn't plummet after the 20th cycle, but sulfur itself violated the green process. In table 1, various other derivatives of graphene (viz. functionalized, non-functionalized, doped, metal composites) had been used over the years to degrade malachite green under visible light irradiation successfully.

Table 1. Tabular representation of the photodegradation of MG with functionalized graphene-based materials.

Material	Dye	pH	Order of the reaction (min^{-1}) MG/MB/MO	Degradation (%)	Adsorption capacity (m^2gm^{-1})	Ref.
ZnO-GO	MG	-	-/-/-	78	-	[39]
TiO_2-GO	MG	-	0.0674/-/-	80	-	[40]
MIL-101-GO	MG	5	-/-/-	92	886	[41]
NiO-GO	MB	8	-/-/-	97.54	-	[42]
GO	MG, MB, R6	-	-/-/-	35.53 (MG), 83(MB)	-	[43]
Fe_3O_4-GO	MG, CV, BG	3	-/-/-	95.6 (MG)	-	[44]
starch-poly(acrylamide)/ GO/hydroxyapatite	MG	5.5	0.0874/-/-	59	297	[45]
ZIF-8/$CoFe_2O_4$/GO	MG	6	0.04836/-/-	98.96	2610	[46]
Corn straw powder/ TiO_2/GO	MG, MB, RB	-	-/0.11497/-	-	242	[47]
Fe_3O_4-GO	MG. MB, MV	6	0.039/0.052/-	-	-	[48]
MnV_{13}/GO/PANI	MG	2	0.01389/-/-	>95	17	[49]
Guar gum/GO	MG, MB, RB	11	-/-/-	98 (MG), 90 (MB)	230 (MG) 227 (MB)	[50]

[1] *MG – Malachite Green, MB – Methylene Blue, MO – Methyl Orange, RB – Rhodamine B, R6 – Rhodamine 6G, CV – Crystal Violet, BG – Brilliant Green, MV – Methyl Violet.

5. Photocatalytic Degradation of Methylene Blue (MB) with Graphene and its Derivatives

The high solubility of methylene blue (MB) in water and alcohols makes it a widely used chemical in textiles and pharmaceutical industries [51]. However, as an *in-vitro* dye usage in photodynamic therapy, biological staining, aquaculture, redox indicator, photosensitizer to generate single oxygen and chromoendoscopy, it is one of the most vital and demanding dyes [52, 53]. In spite of therapeutic values and major clinical applications of MB, it has been a potent threat to human life and aquatic organisms in high dosage. The cytotoxic effects had revealed high concentrations of MB affect proliferation and apoptosis of annulus fibrous cells, as well as several investigations, had shown teratogenic effects on the human fetuses [54, 55]. Hence, removal of MB had been a top priority amongst most commercially available dyes, and the earliest metal-free graphene-based photocatalytic degradation of MB was performed by Sun *et al*. in 2012 [56]. GO, and rGO were used as photocatalysts to degrade phenol and MB under visible light illumination after 3 h.

Peng *et al*. prepared porous rGO to adsorb phenol, and MB was degraded completely after 4 h; however, the concentration of the dye was extremely low ~ 10 ppm [55]. Interestingly,

Fu and co-workers compared Pd-based GO hybrid with metal-free GO in the degradation of MB [54]. In contrast to its metal counterparts, metal-free GO successfully degraded MB within 7 minutes, while its counterparts took 16 minutes. Subsequently, Hu *et al*. used sulfur-based graphene composite to mitigate MB toxicity in water under UV and visible light irradiation in a separate manner [57]. The results were fecund as 99.8% dye broke down in visible light irradiation; however, the toxic effect of sulfur materials cannot be nullified. Liu *et al*. demonstrated the photo-catalytic effects of rGO on 10-ppm MB solution, but the removal process was tedious even for such a low dosage [58].

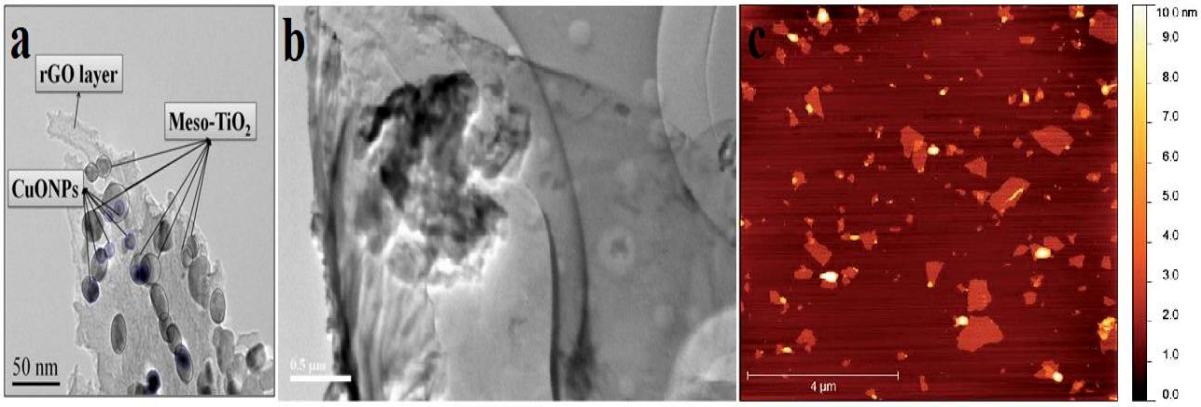

Figure 5. Morphological structures depict the flake-like structures of graphene derivatives stacked upon one another. TEM image of **(a)** CuO-TiO2/rGO nanocatalyst [59] Reprinted with permission from ref [59]. Copyright 2015 Elsevier. TEM image of **(b)** graphitic-C_3N_4/GO hybrids [60]. Reprinted with permission from ref [60]. Copyright 2015 Elsevier. **(c)** AFM image of GO layers [61]. Reprinted with permission from ref [61]. Copyright 2015 Royal Society of Chemistry.

In 2015, Babu *et al*. compared the photocatalytic efficiency of rGO with CuO-TiO_2 nanocomposite in the degradation of MB under diffused sunlight [59]. However, rGO played a crucial role as an adsorbent in removing MB, but the metallic composite degraded the toxic dye more briskly. In Figure 5a, the TEM images clearly illustrated the graphene layers stacked upon one another with TiO_2 and CuO nanoparticles making them a high surface area adsorbent and a promising candidate for MB degradation. On the other hand, to accomplish metal-free photocatalyst, Ai *et al*. fabricated carbon nitride (C_3N_4) blended with graphene in the removal of MB and other organic pollutants from wastewater, herein as depicted in TEM images in Figure 5b, the composite of C_3N_4 – GO also comprised of flake-like structures with high surface area [60]. Interestingly, pure C_3N_4 is more sensitive under UV irradiation, while graphene-based C_3N_4 damaged the dye under visible light illumination within a span of 90 mins. The functionalization of graphene exhibited the oxidation property, and every researcher exploited this ability of graphene in the removal of dyes; hence in a similar trend Song *et al*. exhibited the photo-efficiency of GO degrading MB [61]. The dye adsorbed on the surface of GO ~ 95 %, but this optimal removal required a high amount of photo-catalyst: dye, i.e., 1:3 (Figure 5c). Suresh *et al*. emphasized the green reduction of GO and used clove extract to prepare rGO, exploit the antibacterial properties of rGO, and use it in decolorization of 5 ppm MB solution [62].

A year later, the use of graphene-polyaniline (PANI) metal-free composite was used as a photocatalyst by Neelgund and co-workers in the degradation of MO, MB, and RB [63]. The recyclability of the catalyst showed multiple times usage, but the dye concentration was feeble ~ 10 ppm. The Italians incorporated sulfonated GO on the surface of Nafion members to adsorb cationic dyes, i.e., MO and MB, in darkness as well as in visible light [64]. The experiment

successfully established that GO is a photocatalyst than just a mere adsorbent as degradation was more pronounced in visible light than in darkness. Similarly, Xu *et al*. degraded MB in darkness and under visible light illumination with fabricated wrinkle graphene hybrids blended with porphyrin [65]. The results were promising to confirm the photocatalytic ability of graphene hybrids under visible light. Shinde *et al*. developed metal-free graphene with the doping of sulfur and selenium in the graphitic sheet in the annealing process of GO [66]. The photocatalyst was used in water splitting and degradation of 10 ppm MB; however, the degradation process took over 3.5 h. In 2017, Li and co-workers fabricated rGO polydopamine carbon nitride composite to decolorize 5 ppm MB [67]. Singh *et al*. used soluble graphene nanosheets from petrol soot and used them to remove MB. However, the isolation process gained value-added product as well as showed anti-bacterial activities, but the photocatalyst could degrade low concentration (10 ppm) of dye due to lack of functionalized group in the isolated graphene nanosheet [68, 69].

Liu *et al*. compiled agricultural corn waste with GO as an adsorbent component for MB [70]. Over ~ 414 mg gm^{-1} of the cationic dye adsorbed but was largely dependent on the basic pH environment. Wang *et al*. showed photocatalytic activity of C_3N_4-GO composite in degradation of MB, but the decomposition took nothing less than ~ 4 h [71]. In a similar trend, Yang and co-workers used C_3N_4-rGO nanosheets to degrade MB upon visible light illumination [72]. The degradation efficiency was ~ 79%, but the dye concentration was ~ 10 ppm. Cellulose acetate mixed with GO showed photocatalytic activity on MB and indigo carmine under UV light illumination. However, complete degradation was possible with 10-ppm dye content, but increasing the concentration ~ 60 ppm, there was a drastic fall in degradation efficiency ~ 70 % [73]. On the other hand, B doped GO showed better photodegradation ability than the former, and within 100 and 50 min, it was able to degrade 70% of MO and MB, respectively [74].

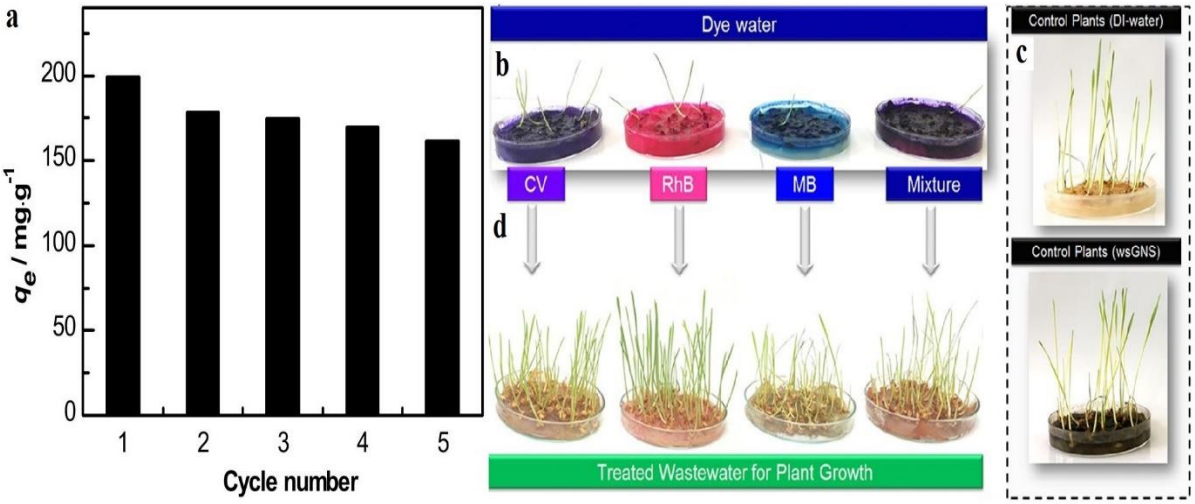

Figure 6. (a) Cyclic adsorption of MB on graphene/carbon nanotube hybrid at 298 K [75] Reprinted with permission from ref [75]. Copyright 2018 Springer Nature. **(b)** The effect of dyes, their mixture versus treated wastewater on the wheat plants was tested for the 15 days of germination; seeds treated with dyes water and their mixture (Crystal Violet + RB + MB); **(c)** control (as in deionized water and in water-soluble Graphene nanosheet solution); versus the **(d)** treated wastewater of dyes and their mixture [76] Reprinted from open-source.

The use of metal-free graphene as adsorbent and photocatalyst increased at a whooping rate since 2019; Huang *et al*. prepared CNT-porous graphene composite to adsorb ~ 232 mg gm^{-1} MB at 328 K [75]. However, the reaction also occurred at room temperature, but the

desorption started after the 5th cycle, as shown in Figure 6a. Singh *et al*. used water-soluble graphene to mitigate a mixture of RB, MB, and crystal violet under visible light and neutral pH conditions. The bio-assay showed the photodegraded wastewater was used to promote sustainable growth in wheat plants, demonstrated in Figure 6b [76]. Das and co-workers pyrolyzed lentils to prepare N-doped graphene and used it to sense ascorbic acid and remove MB within 75 mins [77]. Almost 99% of the blue dye was removed, but this success was limited as dye concentration was ~ 5 ppm and depended on the monochromatic visible light source. Ranjan *et al*. used GO foam to degrade MO, MB, and RB, but the concentration was poor ~ 10 ppm [78]. Interestingly, a high dosage of Congo red and MB was removed (as high as 100 ppm) by Shen and co-workers with GO hydrogel, and micro-organisms encapsulated [79]. Christy *et al*. degraded multicomponent comprising of MB, MG, RB, and Cu^{II} with aminated guar gum – GO hydrogel within 2 h [80]. Over 90% of MB was degraded, but the adsorption depended on a highly acidic environment (pH ~ 3).

Similarly, GO was piled with bentonite clay to form a composite in decolorization of 87% MB by Gogoi and co-workers [81]. The photocatalyst was reused for the 3rd time, but the degradation percentage was reduced to 75. Wang *et al*. reported removal of MB with glycine functionalized rGO; however, the dye content was very low ~ 4 – 12 ppm [82]. The Egyptians assembled porphyrin molecules on GO and used them against 81 and 95% removal of MO and MB, respectively [83]. On the other hand, Fadillah *et al*. used alginate modified GO to remove MB (under 30 mins), but the adsorption relied completely on acidic pH 3 environment [84]. Thus, GO showed spark as a photocatalyst, and thereby metal-free co-catalyst were used to form composites such as tourmaline to counter heavy metal contamination and toxic dye affluents (MB), as shown by Xue and co-workers [85]. On altering the composite ratio, the adsorption capacity attained 454.55 mg gm^{-1} but attained a high concentration of dye ~ 200 ppm; the removal process was hampered. Yue *et al*. reported the synthesis of single-wall CNT-rGO nanocomposite in degradation of MB, which took 1 day to remove 95% of the dye under the electrosorption process [86]. Siong and co-workers solely used metal-free rGO to degrade 98% of MB successfully, but the process was tedious ~ 6 h and involved basic buffer condition ~ pH 11 [87].

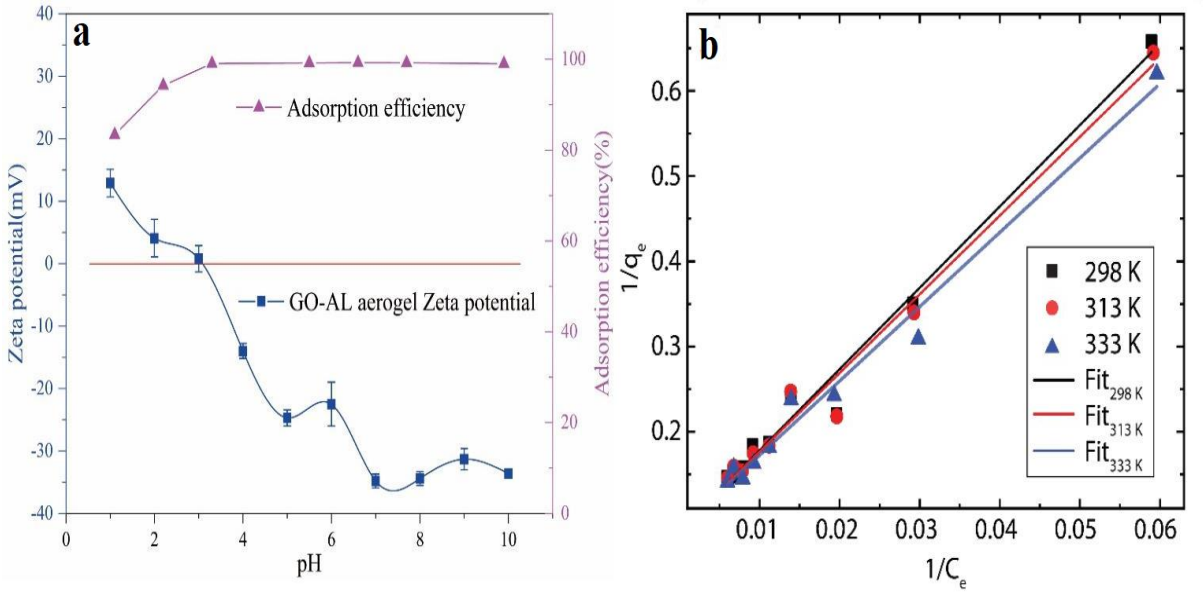

Figure 7. (a) The influence of pH to GO-Alkali/lignin (AL) aerogel adsorb MB and Zeta potential of GO-AL aerogel [88] Reprinted with permission from ref [88]. Copyright 2020 Elsevier. **(b)** Langmuir model adsorption isotherm of MB on rGO at different temperatures [89] Reprinted from Open source.

Recently in 2020, Wu *et al*. prepared a lignin-based GO composite to adsorb a colossal amount of MB (as high as ~ 1186 mg gm^{-1}) under room temperature as well as worked efficiently under neutral pH conditions, as exhibited in figure 7a [88]. Similarly, under pH 7-8, Sharma and co-workers used rGO prepared over high-temperature 500-1100^o C and used it in the removal of MB under 2 h [90]. Mauoche *et al*. prepared N-doped GO aerogel to adsorb MB varying the dye concentration 5-25 ppm; hence the adsorption was higher than GO, but the dye concentration was poor [91]. Arias *et al*. synthesized rGO with a citric acid-reducing agent to promote the eco-friendly process of preparing photocatalyst [89]. Although the synthesis procedure was environmentally benign, the degradation of MB required a high temperature ~ 60^o C, and dye adsorption was moderate, figure 7b. The use of GO on polymeric membrane established high-efficiency removal of organic dyes comprising of mixed dyes, i.e., MB, MO, RB, basic blue, and congo red [92]. Zhang *et al*. constructed a C_3N_4-GO hybrid to remove MB under 3 h, but the purification percentage was comparatively moderate ~ 83% [93]. Earlier the porphyrin-based graphene composite demonstrated metal-free photocatalytic ability, and thereby Ussia and co-workers were compelled to use it in purifying MB contaminating water [94]. The degradation percentage reached ~ 60% after 5 h but the process involved rigorous stirring and bubbling the photocatalyst in the dye solution. Sandhu and co-workers compared the photodegradation quality between GO and rGO in the safe removal of MB solution under UV and visible light irradiation [95]. The results proved that GO was a better catalyst than rGO in the percentage removal of dye under both luminous environments. Therefore, this showed that degradation of high concentration of MB, i.e., ≥ 100 ppm, is quite limited and challenging; hence, it established that functionalized graphene derivative demonstrated photodegradation abilities. In Table 2, photodegradation of MB with various functionalized graphene derivatives comprising metals, ceramics, organic polymers had been represented chronologically.

Table 2. Tabular representation of the photodegradation of MB with functionalized graphene-based materials.

Material	**Dye**	**pH**	**Order of the reaction (min^{-1}) MG/MB/MO**	**Degradation (%)**	**Adsorption capacity (m^2gm^{-1})**	**Ref.**
TiO_2/GO	MB	-	-/0.263/-	70	-	[96]
N-TiO_2/GO	MB	-	-/-/-	66	-	[97]
Fe_3O_4-Gallic acid/ GO	MB	6	-/-/-	100	-	[98]
PVA/ TiO_2/GO	MB,MV	-	-/0.0141/-	95	-	[99]
PVA/GO	MB	-	-/0.833/-	70	-	[100]
TiO_2/GO	MB, MO	7	-/0.268/ 0.00657	100 (MB),84 (MO)	-	[101]
ZnO/polypyrrole/ GO	MB	-	-/0.0011/-	55	-	[102]
Ag_2SO_3/AgBr/ GO	MB, MO, RB	-	-/-/-	88 (MB),99 (MO)	-	[103]
ZnO/GO	MO, CV, CR, NR	7	-/-/0.00616	62.8	-	[104]
TiO_2/Ag/AgCl/GO	MB	-	-/0.0013/-	80	112.6	[105]
TiO_2/GO	MB	-	-/0.0035/-	60	-	[106]
α-Fe_2O_3/GO	MB	2	-/0.1953/-	99	-	[107]
Pd/GO	MB, MO, CR	-	-/-/-	-	2630	[108]
Polythiophene/GO	MB	-	-/0.1149/-	77	-	[109]
Ag_2CrO_4/C_3N_4/GO	MB, RB	-	-/0.04329/-	95	-	[110]
Ag/ZnO/GO	MB	-	-/0.0176/-	97	-	[111]
α-FeOOH/GO	MB	3.1	-/0.0443/-	99	150	[112]
TiO_2/GO	MB	-	-/-/-	92	-	[113]

Material	Dye	pH	Order of the reaction (min^{-1}) MG/MB/MO	Degradation (%)	Adsorption capacity (m^2gm^{-1})	Ref.
$CuFe_2O_4$/ZnO/GO	MB, MO, RB	-	-/-/-	84 (MB), 82 MO)	130	[114]
Ag_3PO_4/GO	MB, RB	-	-/0.75/-	99	-	[115]
Nanodiamond/Pd/ GO	MB	-	-/-/-	90	-	[116]
CeO_2/GO	MB	-	-/0.0266/-	95	41.07	[117]
N-CD/ Ag_3PO_4/GO	MB, RB	-	-/0.6051/-	95	-	[118]
MOF/GO	MB	-	-/-/-	90	-	[119]
CdO/GO	MB, MO, RB	10	-/ 0.044/ 0.029	93.3 (MB), 89 (MO)	-	[120]
Fe-$Ce_2(CO_3)_3$/GO	MB, RB	7	-/0.10036/-	93.72	162.81	[121]
C_3N_4/ GO	MB	-	-/-/-	75	-	[122]
$FePO_4$/ GO	MB	-	-/-/-	50	-	[123]
WO_3/ GO	MB, IC	-	-/-/-	97.03	-	[124]
Polyethylene glycol GO	MB	7	-/0.14/-	91	92.3	[125]
ZnO/GO	MB	-	-/0.0034/-	45	-	[126]
WSe_2/ NGO	MB	-	-/0.0572/-	99.3	-	[127]
Agricultural waste/ GO	MB	12	-/0.10804/-	98.76	414.03	[70]
Cellulose acetate/ GO	MB, IC	2	-/0.006/-	90	-	[73]
Fe-Co_xS_y/ GO	MB, MO, RB	7	-/-/-	100 (MB), 100 (MO)	83.52	[128]
Ag-TiO_2/ GO	MB	-	-/-/-	79.8	-	[129]
$BaTiO_3$/ GO	MB	-	-/0.006/-	80	-	[130]
ZnS/ GO	MB, MO	-	-/-/-	97.1 (MB), 97.6 (MO)	-	[131]
ZnO/GO	MB	6	-/-/-	86.9	42	[132]
NiO/GO	MB	7	-/0.0062/-	97	-	[133]
ZnO/NGO	MB, MO	-	-/0.0251/-	99 (MB), 75 (MO)	42.99	[134]
Ag/P/GO	MB	-	-/0.0313/-	94	-	[135]
TiO_2/GO	MB	4	-/0.052/-	94.98	-	[136]
TiO_2/GO	MB	-	-/-/-	15.9	-	[137]
N- TiO_2/GO	MB	-	-/0.0146/-	80	-	[138]
PVDF/ZnO/GO	MB	9.5	-/0.022/-	86.8	-	[139]
GO	MB, RB	-	-/0.0598/-	-	-	[78]
ZrO_2/GO	MB, RB		-/0.021/-	99.23	46.27	[140]
$MgFe_2O_4$/TiO_2/GO	MB	-	-/0.044/-	95	58.48	[141]
CeO_2/GO	MB	7	-/-/-	81.1	-	[142]
$Zn_{1-x}Ga_xO_{1-y}N_y$/GO	MB	-	-/0.95/-	96	-	[143]
Fe_2O_3/WO_3/GO	MB, CV	-	-/-/-	75	-	[144]
Gd_2O_3/GO	MB	7	-/-/-	99	-	[145]
TiO_2/SnO_2/GO	MB	-	-/0.134/-	99	-	[146]
Bentonite clay/GO	MB	-	-/0.127/-	87	-	[81]
Ag/GO	MB, RB, AY	-	-/0.242/-	98	-	[147]
PAN/ZnO/GO	MB, IC	5	-/-/-	96	-	[148]
AgCl-xGO	MB	-	-/0.989/-	95	-	[149]
Porphyrin-GO	MB, MO	-	-/0.0046/ 0.023	-	-	[83]
Au/Fe_3O_4/dopamine /GO	MB, MO	-	-/00193/-	-	-	[150]
ZnO/CNT/GO	MB	-	-/0.015/-	99	-	[151]
Au/GO	MB, CR, R6	-	-/0.53/-	90	46.4	[152]
$Yb_2(MoO_4)_3$/$YbMoO_4$/GO	MB	3	-/0.0884/-	98	-	[153]
PTh-WSe_2/NGO	MB	-	-/0.02601/-	94.8	-	[154]
TiO_2/GO	MB	-	-/-/-	98.67	91.25	[155]
Cu_2O/GO	MB, RB	-	-/-/-	84	-	[156]
Cellulose/Cu_2O/GO	MB	-	-/-/-	98	-	[157]

Material	Dye	pH	Order of the reaction (min^{-1}) MG/MB/MO	Degradation (%)	Adsorption capacity (m^2gm^{-1})	Ref.
SnO_{2-x}/GO	MO	-	-/-/0.15219	95	-	[158]
Fe_3O_4/GO	MB	3	-/0.0508/-	100	-	[159]
Chitosan/Cellulose/ GO	MB, BG	7	-/0.013/-	100	122.1	[160]
$H_3PW_{12}O_{40}$/GO	MB, MO	-	-/-/-	100 (MB), 100 (MO)	-	[161]
N-ZnO/GO	MB	-	-/-/-	95	-	[162]
$BaTiO_3$/GO	MB	9	-/-/-	95	-	[163]
TiO_2/GO	MB	-	-/0.03393/-	97.5	18.6	[164]
Pt-Co/GO	MB	10	-/-/-	91	273.6	[165]
NiS-In_2O_3/GO	MB	9	-/-/-	97.11	-	[166]
ZnO/SiO_2/GO	MB	9	-/-/-	98	16	[167]
ZnO/GO	MB, MO, RB	-	-/-/-	100 (MB), 100 (MO)	-	[168]
Fe_3O_4/BiOI/GO	MB, RB	-	-/0.0145/-	91.4	-	[169]
Si/GO	MB	-	-/-/-	95	-	[170]
$NiFe_2O_4$/GO	MB	10	-/-/-	90.84	-	[171]
$BiVO_4$/SiO_2/GO	MB	-	-/-/-	95	43.93	[172]
Fe_3O_4/black cumin/ GO	MB	7	-/0.021/-	100	87.71	[173]
TiO_2/GO	MB	10	-/-/-	99	104.51	[174]
$Ca_{10}(PO_4)_6(OH)_2$/Cellulose/ Fe_3O_4/ GO	MB	8	-/0.0703/-	95.1	-	[175]
PEDOT/NaPSS/GO	MB	-	-/-/-	97.9	-	[176]
Nd-MOF/Fe_3O_4/GO	MB	3	-/-/-	95	-	[177]
Cellulose/TiO_2/GO	MB	-	-/-/-	93	-	[178]
Ag/CuO/GO	MB	-	-/0.07414/-	93.11	-	[179]
RuO_2/GO	MB	6	-/-/-	95	-	[180]
Sm_2WO_6/ZnO/GO	MB	-	-/0.4042/-	98.24	-	[181]
$Sm_2(MoO_4)_3$/GO	MB, MO, RB	7	-/-/0.0811	93 (MB), 98 (MO)	-	[182]
$BiVO_4$/PANI/GO	MB	-	-/0.092/-	73	-	[183]
$CoFe_2O_4$/GO	MB, MV	7	-/-/-	92	157	[184]
Cr_2S_3/TiO_2/GO	MB, MO, RB	-	-/0.003/ 0.018	98.3 (MB), 86.3 (MO)	115.8	[185]
Pectin/GO	MB, MO	7	-/0.082/ 0.0108	98 (MB), 87.5 (MO)	-	[186]
$ZnFe_2O_4$/GO	MB	10	-/-/-	90	-	[187]
$Cu_3(btc)_2$/Chitosan/ GO	MB	7	-/0.0529/-	96	947.26	[188]

[1] *IC – Indigo Carmine, CR – Congo Red, AY – Acid Yellow.

6. Photocatalytic Degradation of Methyl Orange (MO) with Graphene and its Derivatives

Methyl orange is a universal indicator involved in various acid-base and redox titrations in quantitative estimation. In forensic science, methyl orange has a significant role in qualitatively determining heroin, morphine, cocaine, codeine, and various other alkaloids in biological fluids [189]. Apart from histological usage as a stain, this azo dye had endless demand as printing textiles, dyeing fabrics, leather, and fibrous paper, making it one of the most necessary commercial dyes in the international market. Despite being an essential coloring material, the detrimental effects of MO are quite adverse on human beings and aquatic life. Among MG, MB, and MO, the latter is the most hazardous and toxicological test that revealed genotoxicity in humans [190, 191].

The degradation of MO with metal-free graphene-based photocatalyst was reported back in 2013 by Peng and Li, both the Chinese researchers who developed sulfur-doped GO [192]. However, the composite wasn't sufficient to break the azo bonds of the dye; thus mere

83% was decolorized after 3 h of reaction. In 2015, Tong *et al*. used graphitic C_3N_4 coupled with GO nanosheets against 20 ppm MO under visible light illumination, and after 4 h, 92% of the dye was removed [190].

A couple of years later, Gong and co-workers prepared GO nanosheets using electrochemical exfoliation, and the material was used to adsorb MO at various pH 2-10. It was found that ~ pH 2 the adsorption was highest ~ 139 mg gm-1, but the catalyst to dye ratio was high [191]. In 2018, Xu *et al*. developed a GO-based membrane filter to purify MO and other dye contents in wastewater with the enzymatic assist. This bio-catalytic approach was quite new, but the relative activity order for MO was quite less than other dyes such as reactive brilliant blue [193]. Wu *et al*. used graphene-like C3N4 nanosheets to adsorb MO on the surface of this porous material with a high surface area ~ 669 m2 gm-1 under a neutral pH environment [194]. Vellaichamy and co-workers in 2019 grafted N-doped graphene on C3N4 and degraded 98.2% within 35 min of irradiation exposure [195]. The photo-catalyst demonstrated remarkable degrading ability at pH 7 even after the 5th cycle, but the dye concentration was ~ 10 ppm and was not used for high concentration trials. Interestingly, the adsorption selectivity of organic dyes on GO surface was shown by Molla and co-workers, consisting of a mixture of three dyes, i.e., MB, RB, and MO [196]. The tuning of electrostatic interactions on the GO surface showed MB and RB adsorption on the photocatalyst's surface while MO was negated from adsorbing. Fang Wang used N - graphene prepared from GO to remove MO from wastewater [197]. The degradation took 5 h with an exiguous ratio of catalyst to dye, i.e., 1:40; however, the concentration of MO was moderate ~ 50 ppm and relied on Xe light source.

Labiadh and Kamali, in 2020, synthesized 3D graphene at various temperatures 300 – 700°C to retain high porosity and active cavity for MO removal adsorption site [198]. In figure 8, it was shown GO prepared after calcination ~ 300°C had the most potential to degrade MO over other variants of GO. The adsorbent not only removed 97.3% MO but was fruitful in degrading MB and congo red into fragments, but the photodegradation assay was done on a moderate dye concentration of 50 ppm. Song *et al*. prepared an anthraquinone-based rGO composite to obliterate 80% MO from an aqueous medium, but the experiments were performed on 5 ppm dye content [199]. Thus, amongst MG, MB, and MO, the removal of MO is quite challenging with metal-free graphene-based materials, and the literature review suggested that breaking the azo-bond of the cationic dye at high concentration needs a high surface area, electrostatic interaction, and active sites in the photo-catalyst.

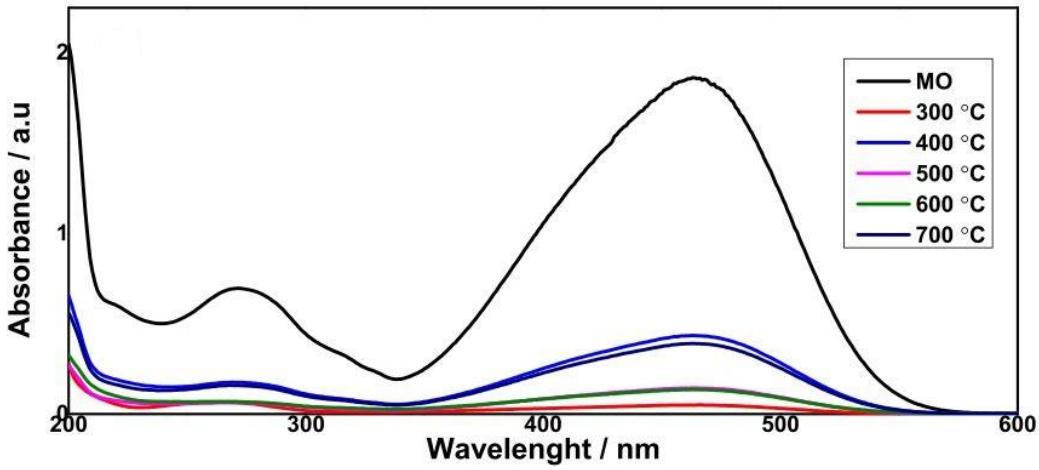

Figure 8. UV–Vis spectra of MO solutions in the presence of regenerated graphene samples after 15 min of adsorption [198]. Reprinted with permission from ref [198]. Copyright 2020 Elsevier.

In Table 3, photodegradation of MO with various graphene derivatives comprising metals, ceramics, and polymeric composites was represented chronologically.

Table 3. Tabular representation of the photodegradation of MO with functionalized graphene-based materials.

Material	Dye	pH	Order of the reaction (min^{-1}) MG/MB/MO	Degradation (%)	Adsorption capacity (m^2gm^{-1})	Ref.
TiO_2/GO	MO	-	-/-/-	35	-	[200]
Fe-MOF/GO	MO	3	-/-/0.0114	98	-	[201]
Ag-Cu_2O/GO	MO	-	-/-/-	90	-	[202]
GO	MO	2	-/-/0.019	88	138.69	[191]
MnO_2/GO	MO	-	-/-/-	93.76	127.5	[203]
TiO_2/ZnO/GO	MO	-	-/-/-	53.8	-	[204]
GO	MO, RS	-	-/-/-	100	-	[205]
Ag_3PO_4/GO	MO	-	-/-/0.00304	90	-	[206]
Ti/GO	MO	3	-/-/-	100	207.6	[207]
Ag_3PO_4/$CoFe_2O_4$/GO	MO	-	-/-/-	91	-	[208]
Fe_3O_4/ZnO/GO	MO	-	-/-/0.0558	92.8	-	[209]
ZnO/GO	MO	7	-/-/0.025	95	-	[210]
CeO_2/GO	MO	-	-/-/0.01488	87	72.68	[211]
Fe_3O_4/ZnO/GO	MO	-	-/-/-	84.87	-	[212]
CD/TiO_2/GO	MO, RB, MB	-	-/-/-	95.54 (MB), 92.47 (MO)	-	[213]
GO	MO	7	-/-/-	65	-	[214]
BiOI/CN/GO	MO	-	-/-/0.051	93	-	[215]
TiO_2/GO	MO	-	-/-/-	45	103	[216]
NiS/MoO_3/GO	MO	4	-/-/-	97	-	[217]
CuO/Cu_2O/GO	MO	-	-/-/0.01	95	-	[218]
Gd_2O_3/Bi_2O_3/GO	MO	6	-/-/0.028	95	544	[219]
Cu_2O/Cu/GO	MO	-	-/-/-	93	20	[220]
N-CD/WO_3/GO	MO	-	-/-/-	77	-	[221]
TiO_2/GO	MO	-	-/-/-	90	152.5	[222]
Co_3O_4/TiO_2/GO	MO	-	-/-/-	96	-	[223]
TiO_2/GO	MO, CR	7	-/-/0.0631	84	92	[224]
AgI/Bi_2O_3/GO	MO	-	-/-/0.041	98	24	[225]
NGO	MG, MB, MO	7	0.082/0.00233/ 0.00313	95 (MG), 97.9 (MB), 99.6 (MO)	-	[226]
GQD	MB, MO	8	-/0.01133/0.00519	79.4 (MB), 52 (MO)	-	[227]

7. Conclusions

The extraordinarily high surface area, zero bandgap nature, and many conjugated (-bonds proved graphene to be a promising candidate for the degradation of carcinogenic pollutants in water. Multiple graphenes and their numerous hybrids had been used against the successful removal of malachite green (MG), methylene blue (MB), and methyl orange (MO), as summarized in this review. Chronological studies have revealed the importance of doping, mixing, and loading various components with functionalized graphene helped boost the degradation efficiency against these pollutant dyes. The poly-aromatic resonating π-system of graphene oxide (GO) and reduced graphene oxide (rGO) were initiated a free radical mechanism with the conjugated dye molecules via electrostatic interactions, hydrogen bonding, π-π stacking and oxidative photonic interactions. The hydrophilic nature of GO and rGO vastly augments their ability to interact with these pollutant dyes via adsorption or chemical interaction leading to the breakdown of these high resonances stabilized dye molecules.

Various adsorption isotherm models viz. Temkin, Langmuir, Freundlich proposed the pseudo-1st order kinetics between the adsorbing graphene structure and the pollutant dyes. Certain cases have shown graphene-based photodegrading materials had high recovery and recycling abilities than their metallic counterparts. Thus in upcoming years, it is highly anticipated high-quality, defect-free, functionalized graphene and its derivatives might be obtained via chemical synthesis route for the mitigation of these agricultural, pharmaceutical, and industrial effluents in a broad-scale pragmatic way.

Funding

This work was self-funded by the authors.

Acknowledgments

The authors like to thank the Department of Chemistry, NIT – Agartala, and the Indian Institute of Science Education and Research (IISER) – Kolkata for granting us access to the Web of Science database.

Conflicts of Interest

The authors declare no conflict of interest.

References

1. Hummers Jr, W. S.; Offeman, R. E. Preparation of graphitic oxide. *J. Am. Chem. Soc.* **1958,** *80*, 1339-1339, https://doi.org/10.1021/ja01539a017.
2. Marcano, D. C.; Kosynkin, D. V.; Berlin, J. M.; Sinitskii, A.; Sun, Z.; Slesarev, A. S.; Alemany, L. B.; Lu, W.; Tour, J. M. Correction to improved synthesis of graphene oxide. *ACS Nano* **2018,** *12* , 2078-2078, https://doi.org/10.1021/nn1006368.
3. Biswas, R.; Bharali, N.; Neog, A., A Novel Route towards Sustainable Synthesis of Graphene. *Lett. Appl. Nanobioscience*, **2021**, *10*, 2760 – 2765, https://doi.org/10.33263/LIANBS104.27602765.
4. Mandal, P.; Saha, M. Scalable preparation of carbon nanoparticles and graphene nanoflakes using sand paper abrasion. *Materialwiss. Werkst.* **2020,** *51*, 902-907, https://doi.org/10.1002/mawe.201900135.
5. Dong, Y.; Shao, J.; Chen, C.; Li, H.; Wang, R.; Chi, Y.; Lin, X.; Chen, G. Blue luminescent graphene quantum dots and graphene oxide prepared by tuning the carbonization degree of citric acid. *Carbon* **2012,** *50*, 4738-4743, https://doi.org/10.1016/j.carbon.2012.06.002.
6. Yang, X.; Dou, X.; Rouhanipour, A.; Zhi, L.; Räder, H. J.; Müllen, K. Two-dimensional graphene nanoribbons. *J. Am. Chem. Soc.* **2008,** *130* , 4216-4217. https://doi.org/10.1021/ja710234t.
7. Li, G.; Yoon, K. Y.; Zhong, X.; Zhu, X.; Dong, G. Efficient Bottom-Up Preparation of Graphene Nanoribbons by Mild Suzuki–Miyaura Polymerization of Simple Triaryl Monomers. *Chem. Eur. J.* **2016,** *22*, 9116-9120, https://doi.org/10.1002/chem.201602007.
8. Li, G.; Yoon, K.-Y.; Zhong, X.; Wang, J.; Zhang, R.; Guest, J. R.; Wen, J.; Zhu, X.-Y.; Dong, G. A modular synthetic approach for band-gap engineering of armchair graphene nanoribbons. *Nat. Commun.* **2018,** *9*, 1-9, https://doi.org/10.1038/s41467-018-03747-2.
9. El Gemayel, M.; Narita, A.; Dössel, L. F.; Sundaram, R. S.; Kiersnowski, A.; Pisula, W.; Hansen, M. R.; Ferrari, A. C.; Orgiu, E.; Feng, X. Graphene nanoribbon blends with P3HT for organic electronics. *Nanoscale* **2014,** *6*, 6301-6314, https://doi.org/10.1039/C4NR00256C.
10. Huang, Y.; Xu, F.; Ganzer, L.; Camargo, F. V.; Nagahara, T.; Teyssandier, J.; Van Gorp, H.; Basse, K.; Straasø, L. A.; Nagyte, V. Intrinsic properties of single graphene nanoribbons in solution: synthetic and spectroscopic studies. *J. Am. Chem. Soc.* **2018,** *140*, 10416-10420, https://doi.org/10.1021/jacs.8b06028.
11. Pawlak, R.; Liu, X.; Ninova, S.; D'Astolfo, P.; Drechsel, C.; Sangtarash, S.; Häner, R.; Decurtins, S.; Sadeghi, H.; Lambert, C. J. Bottom-up synthesis of nitrogen-doped porous graphene nanoribbons. *J. Am. Chem. Soc.* **2020,** *142*, 12568-12573, https://doi.org/10.1021/jacs.0c03946.

12. Jacobse, P. H.; McCurdy, R. D.; Jiang, J.; Rizzo, D. J.; Veber, G.; Butler, P.; Zuzak, R.; Louie, S. G.; Fischer, F. R.; Crommie, M. F. Bottom-up Assembly of Nanoporous Graphene with Emergent Electronic States. *J. Am. Chem. Soc.* **2020,** *142*, 13507-13514, https://doi.org/10.1021/jacs.0c05235.
13. Hein, S. J.; Lehnherr, D.; Arslan, H.; J. Uribe-Romo, F.; Dichtel, W. R. Alkyne benzannulation reactions for the synthesis of novel aromatic architectures. *Acc. Chem. Res.* **2017,** *50*, 2776-2788, https://doi.org/10.1021/acs.accounts.7b00385.
14. Mandal, P.; Debbarma, J.; Saha, M. One Step Synthesis of N-Containing Graphene Oxide from 3-Aminophenol. *Cryst. Res. Technol.* **2020,** *55*, 1900158, https://doi.org/10.1002/crat.201900158.
15. Mandal, P.; Saha, M. Low-temperature synthesis of graphene derivatives: mechanism and characterization. *Chem. Pap.* **2019,** *73*, 1997-2006, https://doi.org/10.1007/s11696-019-00756-3.
16. Selvaraj, V.; Karthika, T. S.; Mansiya, C.; Alagar, M. An over review on recently developed techniques, mechanisms and intermediate involved in the advanced azo dye degradation for industrial applications. *J. Mol. Struct.* **2020**, 129195, https://doi.org/10.1016/j.molstruc.2020.129195.
17. Kumar, R.; Sankhla, M.S.; Kumar, R.; Sonone, S.S. Impact of Pesticide Toxicity in Aquatic Environment. *Biointerface Res.Appl. Chem*. **2021**, *11*, 10131-10140, https://doi.org/10.33263/BRIAC113.1013110140.
18. Song, J.; Han, G.; Wang, Y.; Jiang, X.; Zhao, D.; Li, M.; Yang, Z.; Ma, Q.; Parales, R. E.; Ruan, Z. pathway and kinetics of malachite green biodegradation by Pseudomonas veronii. *Sci. Rep.* **2020,** *10*, 1-11, https://doi.org/10.1038/s41598-020-61442-z.
19. Mustapha, R.; Ali, A.; Subramaniam, G.; Zuki, A.A.A.; Awang, M.; Harun, M.H.C.; Hamzah, S. Removal of Malachite Green Dye Using Oil Palm Empty Fruit Bunch as a Low-Cost Adsorbent. *Biointerface Res. Appl. Chem.* **2021**, *11*, 14998-15008, https://doi.org/10.33263/BRIAC116.1499815008.
20. Mishra, S.P.; Patra, A.R.; Das, S. Methylene blue and malachite green removal from aqueous solution using waste activated carbon. *Biointerface Res. Appl. Chem*. **2020**, *11*, 7410-7421. https://doi.org/10.33263/BRIAC111.74107421.
21. Chowdhury, S.; Mishra, R.; Saha, P.; Kushwaha, P. Adsorption thermodynamics, kinetics and isosteric heat of adsorption of malachite green onto chemically modified rice husk. *Desalination* **2011,** *265*, 159-168, https://doi.org/10.1016/j.desal.2010.07.047.
22. Sharma, P.; Das, M. R. Removal of a cationic dye from aqueous solution using graphene oxide nanosheets: investigation of adsorption parameters. *J. Chem. Eng. Data* **2013,** *58*, 151-158, https://doi.org/10.1021/je301020n.
23. Zhang, X.; Yu, H.; Yang, H.; Wan, Y.; Hu, H.; Zhai, Z.; Qin, J. Graphene oxide caged in cellulose microbeads for removal of malachite green dye from aqueous solution. *J. Colloid Interface Sci.* **2015,** *437*, 277-282, https://doi.org/10.1016/j.jcis.2014.09.048.
24. Suresh, D.; Kumar, M. P.; Nagabhushana, H.; Sharma, S. Cinnamon supported facile green reduction of graphene oxide, its dye elimination and antioxidant activities. *Mat. Lett.* **2015,** *151*, 93-95, https://doi.org/10.1016/j.matlet.2015.03.035.
25. Upadhyay, R. K.; Soin, N.; Bhattacharya, G.; Saha, S.; Barman, A.; Roy, S. S. Grape extract assisted green synthesis of reduced graphene oxide for water treatment application. *Mat. Lett.* **2015,** *160*, 355-358, https://doi.org/10.1016/j.matlet.2015.07.144.
26. Jayanthi, S.; Eswar, N. K.; Singh, S. A.; Chatterjee, K.; Madras, G.; Sood, A., Macroporous three-dimensional graphene oxide foams for dye adsorption and antibacterial applications. *RSC Adv.* **2016,** *6*, 1231-1242, https://doi.org/10.1039/C5RA19925E.
27. Rathour, R.; Das, P.; Aikat, K. Microwave-assisted synthesis of graphene and its application for adsorptive removal of malachite green: thermodynamics, kinetics and isotherm study. *Desalin. Water Treat.* **2016,** *57*, 7312-7321, https://doi.org/10.1080/19443994.2015.1020507.
28. Robati, D.; Rajabi, M.; Moradi, O.; Najafi, F.; Tyagi, I.; Agarwal, S.; Gupta, V. K. Kinetics and thermodynamics of malachite green dye adsorption from aqueous solutions on graphene oxide and reduced graphene oxide. *J. Mol. Liq.* **2016,** *214*, 259-263, https://doi.org/10.1016/j.molliq.2015.12.073.
29. Shi, Y.-C.; Wang, A.-J.; Wu, X.-L.; Chen, J.-R.; Feng, J.-J. Green-assembly of three-dimensional porous graphene hydrogels for efficient removal of organic dyes. *J. Colloid Interface Sci.* **2016,** *484*, 254-262, https://doi.org/10.1016/j.jcis.2016.09.008.
30. Gupta, K.; Khatri, O. P. Reduced graphene oxide as an effective adsorbent for removal of malachite green dye: Plausible adsorption pathways. *J. Colloid Interface Sci.* **2017,** *501*, 11-21, https://doi.org/10.1016/j.jcis.2017.04.035.

31. Wei, S.-C.; Fan, S.; Lien, C.-W.; Unnikrishnan, B.; Wang, Y.-S.; Chu, H.-W.; Huang, C.-C.; Hsu, P.-H.; Chang, H.-T. Graphene oxide membrane as an efficient extraction and ionization substrate for spray-mass spectrometric analysis of malachite green and its metabolite in fish samples. *Anal. Chim. Acta* **2018,** *1003*, 42-48, https://doi.org/10.1016/j.aca.2017.11.076.
32. Sykam, N.; Madhavi, V.; Rao, G. M. Rapid and efficient green reduction of graphene oxide for outstanding supercapacitors and dye adsorption applications. *J. Environ. Chem. Eng.* **2018,** *6*, 3223-3232, https://doi.org/10.1016/j.jece.2018.05.003.
33. Xing, X.; Zhang, X.; Zhang, K.; Jin, L. e.; Cao, Q. Preparation of large-sized graphene from needle coke and the adsorption for malachite green with its graphene oxide. *Fuller. Nanotub. Car. N.* **2019,** *27*, 97-105, https://doi.org/10.1080/1536383X.2018.1512099.
34. Tang, S.; Xia, D.; Yao, Y.; Chen, T.; Sun, J.; Yin, Y.; Shen, W.; Peng, Y. Dye adsorption by self-recoverable, adjustable amphiphilic graphene aerogel. *J. Colloid Interface Sci.* **2019,** *554*, 682-691, https://doi.org/10.1016/j.jcis.2019.07.041.
35. Wang, G.; Li, G.; Huan, Y.; Hao, C.; Chen, W. Acrylic acid functionalized graphene oxide: High-efficient removal of cationic dyes from wastewater and exploration on adsorption mechanism. *Chemosphere* **2020,** *261*, 127736, https://doi.org/10.1016/j.chemosphere.2020.127736.
36. Chen, H.; Liu, T.; Meng, Y.; Cheng, Y.; Lu, J.; Wang, H. Novel graphene oxide/aminated lignin aerogels for enhanced adsorption of malachite green in wastewater. *Colloids Surf. A Physicochem. Eng. Asp.* **2020,** *603*, 125281, https://doi.org/10.1016/j.colsurfa.2020.125281.
37. Söğüt, E. G.; Karataş, Y.; Gülcan, M.; Kılıç, N. Ç. Enhancement of adsorption capacity of reduced graphene oxide by sulfonic acid functionalization: Malachite green and Zn (II) uptake. *Mat. Chem. Phys.* **2020,** *256*, 123662, https://doi.org/10.1016/j.matchemphys.2020.123662.
38. Wang, Y.; Cui, X.; Wang, Y.; Shan, W.; Lou, Z.; Xiong, Y. A thiourea cross-linked three-dimensional graphene aerogel as a broad-spectrum adsorbent for dye and heavy metal ion removal. *New J. Chem.* **2020,** *44*, 16285-16293, https://doi.org/10.1039/D0NJ03345F.
39. Herring, N. P.; Almahoudi, S. H.; Olson, C. R.; El-Shall, M. S. Enhanced photocatalytic activity of ZnO–graphene nanocomposites prepared by microwave synthesis. *J. Nanoparticle Res.* **2012,** *14* , 1-13, https://doi.org/10.1007/s11051-012-1277-7.
40. Perera, S. D.; Mariano, R. G.; Vu, K.; Nour, N.; Seitz, O.; Chabal, Y.; Balkus Jr, K. J. Hydrothermal synthesis of graphene-TiO2 nanotube composites with enhanced photocatalytic activity. *ACS Catal.* **2012,** *2*, 949-956, https://doi.org/10.1021/cs200621c.
41. Fazaeli, R.; Aliyan, H.; Banavandi, R. S. Sunlight assisted photodecolorization of malachite green catalyzed by MIL-101/graphene oxide composites. *Russ. J. Appl. Chem.* **2015,** *88*, 169-177, https://doi.org/10.1134/S1070427215010243.
42. Rong, X.; Qiu, F.; Zhang, C.; Fu, L.; Wang, Y.; Yang, D. Adsorption–photodegradation synergetic removal of methylene blue from aqueous solution by NiO/graphene oxide nanocomposite. *Powder Technol.* **2015,** *275*, 322-328, https://doi.org/10.1016/j.powtec.2015.01.079.
43. Chaudhary, R. P.; Pawar, P. B.; Vaibhav, K.; Saxena, S.; Shukla, S. Quantification of adsorption of azo dye molecules on graphene oxide using optical spectroscopy. *JOM* **2017,** *69*, 236-240, https://doi.org/10.1007/s11837-016-2172-y.
44. Chen, J.; Leng, J.; Yang, X.; Liao, L.; Liu, L.; Xiao, A. Enhanced performance of magnetic graphene oxide-immobilized laccase and its application for the decolorization of dyes. *Molecules* **2017,** *22*, 221. https://doi.org/10.3390/molecules22020221.
45. Hosseinzadeh, H.; Ramin, S. Fabrication of starch-graft-poly (acrylamide)/graphene oxide/hydroxyapatite nanocomposite hydrogel adsorbent for removal of malachite green dye from aqueous solution. *Int. J. Biol. Marcomol.* **2018,** *106*, 101-115, https://doi.org/10.1016/j.ijbiomac.2017.07.182.
46. Mahmoodi, N. M.; Oveisi, M.; Bakhtiari, M.; Hayati, B.; Shekarchi, A. A.; Bagheri, A.; Rahimi, S. Environmentally friendly ultrasound-assisted synthesis of magnetic zeolitic imidazolate framework-Graphene oxide nanocomposites and pollutant removal from water. *J. Mol. Liq.* **2019,** *282*, 115-130, https://doi.org/10.1016/j.molliq.2019.02.139.
47. Chen, J.; Liu, S.; Ge, H.; Zou, Y. A hydrophobic bio-adsorbent synthesized by nanoparticle-modified graphene oxide coated corn straw pith for dye adsorption and photocatalytic degradation. *Environ. Technol.* **2020,** *41*, 3633-3645, https://doi.org/10.1080/09593330.2019.1616827.

48. Akrami, M.; Danesh, S.; Eftekhari, M., Comparative study on the removal of cationic dyes using different graphene oxide forms. *J. Inorg. Organomet. Polym. Mater.* **2019,** *29*, 1785-1797, https://doi.org/10.1007/s10904-019-01140-0.
49. Zhang, C.-L.; Ma, R.-H. Synthesis and photocatalytic activity of MnV13/GO/PANI composite catalysts. *J. Coord. Chem.* **2019,** *72*, 2735-2748, https://doi.org/10.1080/00958972.2019.1670816.
50. Gopi, S.; Rajeswari, A.; Sudharsan, G.; Pius, A. Highly crosslinked 3-D hydrogels based on graphene oxide for enhanced remediation of multi contaminant wastewater. *J. Water Process. Eng.* **2019,** *31*, 100850, https://doi.org/10.1016/j.jwpe.2019.100850.
51. Zayed, M.; Othman, H.; Ghazal, H.; Hassabo, A. G. Psidium Guajava Leave Extract as Reducing Agent for Synthesis of Zinc Oxide Nanoparticles and Its Application to Impart Multifunctional Properties for Cellulosic Fabrics. *Biointerface Res. Appl. Chem.* **2021,** *11*, 13535-13556, https://doi.org/10.33263/BRIAC115.1353513556.
52. Elazab, H.A.; Okasha, A.O.; Radwan, M.A.; Sadek, M.A.; Firouzi, A.; Tamer, T. Removal of Methylene Blue by Adsorption of Water Hyacinth Derived Active Carbon Embedded with Cobalt Nanoparticles. *Lett. Appl. Nanobioscience* **2021**, *10*, 2697 – 2705, https://doi.org/10.33263/LIANBS104.26972705.
53. Verma, R.K.; Sankhla, M.S.; Rathod, N.V.; Sonone, S.S.; Parihar, K.; Singh, G.K. Eradication of Fatal Textile Industrial Dyes by Wastewater Treatment. *Biointerface Res. Appl. Chem.* **2022**, *12*, 567 – 587, https://doi.org/10.33263/BRIAC121.567587.
54. Fu, G.; Tao, L.; Zhang, M.; Chen, Y.; Tang, Y.; Lin, J.; Lu, T. One-pot, water-based and high-yield synthesis of tetrahedral palladium nanocrystal decorated graphene. *Nanoscale* **2013,** *5*, 8007-8014, https://doi.org/10.1039/C3NR02179C.
55. Peng, W.; Liu, S.; Sun, H.; Yao, Y.; Zhi, L.; Wang, S. Synthesis of porous reduced graphene oxide as metal-free carbon for adsorption and catalytic oxidation of organics in water. *J. Mater. Chem. A* **2013,** *1*, 5854-5859, https://doi.org/10.1039/C3TA10592J.
56. Sun, H.; Liu, S.; Zhou, G.; Ang, H. M.; Tadé, M. O.; Wang, S. Reduced graphene oxide for catalytic oxidation of aqueous organic pollutants. *ACS Appl. Mater. Interfaces* **2012,** *4*, 5466-5471, https://doi.org/10.1021/am301372d.
57. Hu, C.; Zheng, S.; Lian, C.; Chen, F.; Lu, T.; Hu, Q.; Duo, S.; Zhang, R. One-step synthesis of a sulfur–graphene composite with enhanced photocatalytic performance. *Appl. Surf. Sci.* **2014,** *314*, 266-272, https://doi.org/10.1016/j.apsusc.2014.06.119.
58. Liu, S.; Peng, W.; Sun, H.; Wang, S. Physical and chemical activation of reduced graphene oxide for enhanced adsorption and catalytic oxidation. *Nanoscale* **2014,** *6*, 766-771, https://doi.org/10.1039/C3NR04282K.
59. Babu, S. G.; Vinoth, R.; Neppolian, B.; Dionysiou, D. D.; Ashokkumar, M. Diffused sunlight driven highly synergistic pathway for complete mineralization of organic contaminants using reduced graphene oxide supported photocatalyst. *J. Hazard. Mater.* **2015,** *291*, 83-92, https://doi.org/10.1016/j.jhazmat.2015.02.071.
60. Ai, B.; Duan, X.; Sun, H.; Qiu, X.; Wang, S. Metal-free graphene-carbon nitride hybrids for photodegradation of organic pollutants in water. *Catal. Today* **2015,** *258*, 668-675, https://doi.org/10.1016/j.cattod.2015.01.024.
61. Song, S.; Ma, Y.; Shen, H.; Zhang, M.; Zhang, Z., Removal and recycling of ppm levels of methylene blue from an aqueous solution with graphene oxide. *RSC Adv.* **2015,** *5*, 27922-27932, https://doi.org/10.1039/C4RA16982D.
62. Suresh, D.; Nagabhushana, H.; Sharma, S. Clove extract mediated facile green reduction of graphene oxide, its dye elimination and antioxidant properties. *Mater. Lett.* **2015,** *142*, 4-6, https://doi.org/10.1016/j.matlet.2014.11.073.
63. Neelgund, G. M.; Bliznyuk, V. N.; Oki, A. Photocatalytic activity and NIR laser response of polyaniline conjugated graphene nanocomposite prepared by a novel acid-less method. *Appl. Catal. B. Environ.* **2016,** *187*, 357-366, https://doi.org/10.1016/j.apcatb.2016.01.009.
64. Scalese, S.; Nicotera, I.; D'Angelo, D.; Filice, S.; Libertino, S.; Simari, C.; Dimos, K.; Privitera, V. Cationic and anionic azo-dye removal from water by sulfonated graphene oxide nanosheets in Nafion membranes. *New J. Chem.* **2016,** *40*, 3654-3663, https://doi.org/10.1039/C5NJ03096J.
65. Xu, H.; Xiang, J. X.; Wu, P.; Lu, Y. F.; Zhang, S.; Xie, Z. Y.; Gu, Z. Z. Synthesis of wrinkled graphene hybrids for enhanced visible-light photocatalytic activities. *RSC Adv.* **2016,** *6*, 45617-45623, https://doi.org/10.1039/C6RA01458E.

66. Shinde, S.; Sami, A.; Lee, J.-H. Sulfur mediated graphitic carbon nitride/S-Se-graphene as a metal-free hybrid photocatalyst for pollutant degradation and water splitting. *Carbon* **2016,** *96*, 929-936, https://doi.org/10.1016/j.carbon.2015.10.050.
67. Li, F.; Yu, Z.; Shi, H.; Yang, Q.; Chen, Q.; Pan, Y.; Zeng, G.; Yan, L. A Mussel-inspired method to fabricate reduced graphene oxide/g-C3N4 composites membranes for catalytic decomposition and oil-in-water emulsion separation. *Chem. Eng. J.* **2017,** *322*, 33-45, https://doi.org/10.1016/j.cej.2017.03.145.
68. Singh, A.; Khare, P.; Verma, S.; Bhati, A.; Sonker, A. K.; Tripathi, K. M.; Sonkar, S. K. Pollutant soot for pollutant dye degradation: soluble graphene nanosheets for visible light induced photodegradation of methylene blue. *ACS Sustain. Chem. Eng.* **2017,** *5*, 8860-8869, https://doi.org/10.1021/acssuschemeng.7b01645.
69. Khare, P.; Singh, A.; Verma, S.; Bhati, A.; Sonker, A. K.; Tripathi, K. M.; Sonkar, S. K. Sunlight-induced selective photocatalytic degradation of methylene blue in bacterial culture by pollutant soot derived nontoxic graphene nanosheets. *ACS Sustain. Chem. Eng.* **2018,** *6*, 579-589, https://doi.org/10.1021/acssuschemeng.7b02929.
70. Liu, S.; Ge, H.; Wang, C.; Zou, Y.; Liu, J. Agricultural waste/graphene oxide 3D bio-adsorbent for highly efficient removal of methylene blue from water pollution. *Sci. Total Environ.* **2018,** *628*, 959-968, https://doi.org/10.1016/j.scitotenv.2018.02.134.
71. Wang, H.; Shen, Q.; You, Z.; Su, Y.; Yu, Y.; Babapour, A.; Zhang, F.; Cheng, D.; Yang, H. Preparation of nanoscale-dispersed g-C3N4/graphene oxide composite photocatalyst with enhanced visible-light photocatalytic activity. *Mater. Lett.* **2018,** *217*, 143-145, https://doi.org/10.1016/j.matlet.2018.01.037.
72. Yang, Y.; Zhao, H.; Yang, H.; Qiu, P.; Zhou, B.; Zhang, N. *In situ* fabrication of reduced graphene oxide/mesoporous g-C3N4 nanosheets with excellent visible light activity. *J. Environ. Chem. Eng.* **2018,** *6*, 890-897, https://doi.org/10.1016/j.jece.2018.01.019.
73. Aboamera, N. M.; Mohamed, A.; Salama, A.; Osman, T.; Khattab, A. An effective removal of organic dyes using surface functionalized cellulose acetate/graphene oxide composite nanofibers. *Cellulose* **2018,** *25*, 4155-4166, https://doi.org/10.1007/s10570-018-1870-8.
74. Singh, M.; Kaushal, S.; Singh, P.; Sharma, J., Boron doped graphene oxide with enhanced photocatalytic activity for organic pollutants. *J. Photochem. Photobiol. A Chem.* **2018,** *364*, 130-139, https://doi.org/10.1016/j.jphotochem.2018.06.002.
75. Huang, Y.; Zhu, J.; Liu, H.; Wang, Z.; Zhang, X. Preparation of porous graphene/carbon nanotube composite and adsorption mechanism of methylene blue. *SN Appl. Sci.* **2019,** *1*, 1-11, https://doi.org/10.1007/s42452-018-0035-6.
76. Singh, A.; Bhati, A.; Khare, P.; Tripathi, K. M.; Sonkar, S. K. Soluble graphene nanosheets for the sunlight-induced photodegradation of the mixture of dyes and its environmental assessment. *Sci. Rep.* **2019,** *9* , 1-12, https://doi.org/10.1038/s41598-019-38717-1.
77. Das, G. S.; Tripathi, K. M.; Kumar, G.; Paul, S.; Mehara, S.; Bhowmik, S.; Pakhira, B.; Sarkar, S.; Roy, M.; Kim, T. Nitrogen-doped fluorescent graphene nanosheets as visible-light-driven photocatalysts for dye degradation and selective sensing of ascorbic acid. *New J. Chem.* **2019,** *43*, 14575-14583, https://doi.org/10.1039/C9NJ02344E.
78. Ranjan, P.; Verma, P.; Agrawal, S.; Rao, T. R.; Samanta, S. K.; Thakur, A. D. Inducing dye-selectivity in graphene oxide for cationic dye separation applications. *Mater. Chem. Phys.* **2019,** *226*, 350-355, https://doi.org/10.1016/j.matchemphys.2019.01.047.
79. Shen, L.; Jin, Z.; Xu, W.; Jiang, X.; Shen, Y.-x.; Wang, Y.; Lu, Y. Enhanced treatment of anionic and cationic dyes in wastewater through live bacteria encapsulation using graphene hydrogel. *Ind. Eng. Chem. Res.* **2019,** *58*, 7817-7824, https://doi.org/10.1021/acs.iecr.9b01950.
80. Gopi, S.; Rajeswari, A.; Sudharsan, G.; Pius, A. Highly crosslinked 3-D hydrogels based on graphene oxide for enhanced remediation of multi contaminant wastewater. *J. Water Process Eng.* **2019,** *31*, 100850, https://doi.org/10.1016/j.jwpe.2019.100850.
81. Gogoi, J.; Choudhury, A. D.; Chowdhury, D. Graphene oxide clay nanocomposite as an efficient photo-catalyst for degradation of cationic dye. *Mater. Chem. Phys.* **2019,** *232*, 438-445, https://doi.org/10.1016/j.matchemphys.2019.05.010.
82. Wang, C.; Ma, G.; Zhou, J.; Zhang, M.; Ma, X.; Duo, F.; Chu, L.; Huang, J.; Su, X. Glycine-functionalized reduced graphene oxide for methylene blue removal. *Appl. Organomet. Chem.* **2019,** *33*, e5077. https://doi.org/10.1002/aoc.5077.

83. El-Shafai, N.; El-Khouly, M. E.; El-Kemary, M.; Ramadan, M. S.; Masoud, M. S. Self-assembly of porphyrin on graphene oxide in aqueous medium: fabrication, characterization, and photocatalytic studies. *Photochem. Photobiol. Sci.* **2019,** *18*, 2071-2079, https://doi.org/10.1039/C9PP00088G.
84. Fadillah, G.; Saleh, T. A.; Wahyuningsih, S.; Putri, E. N. K.; Febrianastuti, S. Electrochemical removal of methylene blue using alginate-modified graphene adsorbents. *Chem. Eng. J.* **2019,** *378*, 122140, https://doi.org/10.1016/j.cej.2019.122140.
85. Xue, G.; Luo, X.; Srinivasakannan, C.; Zheng, L.; Miao, Y.; Duan, X. Effective removal of organic dye and heavy metal from wastewater by tourmaline/graphene oxide composite nano material. *Mater. Res. Express* **2019,** *6*, 115618, https://doi.org/10.1088/2053-1591/ab4d22.
86. Yue, F.; Zhang, Q.; Xu, L.; Zheng, Y.; Yao, C.; Jia, J.; Leng, W.; Hou, S. Porous reduced graphene oxide/single-walled carbon nanotube film as freestanding and flexible electrode materials for electrosorption of organic dye. *ACS Appl. Nano Mater.* **2019,** *2*, 6258-6267, https://doi.org/10.1021/acsanm.9b01236.
87. Siong, V. L. E.; Lee, K. M.; Juan, J. C.; Lai, C. W.; Tai, X. H.; Khe, C. S. Removal of methylene blue dye by solvothermally reduced graphene oxide: a metal-free adsorption and photodegradation method. *RSC Adv.* **2019,** *9*, 37686-37695, https://doi.org/10.1039/C9RA05793E.
88. Wu, Z.; Huang, W.; Shan, X.; Li, Z. Preparation of a porous graphene oxide/alkali lignin aerogel composite and its adsorption properties for methylene blue. *Int. J. Biol. Marcomol.* **2020,** *143*, 325-333, https://doi.org/10.1016/j.ijbiomac.2019.12.017.
89. Arias Arias, F.; Guevara, M.; Tene, T.; Angamarca, P.; Molina, R.; Valarezo, A.; Salguero, O.; Vacacela Gomez, C.; Arias, M.; Caputi, L. S., The adsorption of methylene blue on eco-friendly reduced graphene oxide. *Nanomaterials* **2020,** *10*, 681, https://doi.org/10.3390/nano10040681.
90. Sharma, A.; Erdenedelger, G.; Jeong, H. M.; Lee, B.-K. Controlled oxygen functional groups on reduced graphene using rate of temperature for advanced sorption process. *J. Environ. Chem. Eng.* **2020,** *8*, 103749, https://doi.org/10.1016/j.jece.2020.103749.
91. Maouche, C.; Zhou, Y.; Peng, J.; Wang, S.; Sun, X.; Rahman, N.; Yongphet, P.; Liu, Q.; Yang, J. A 3D nitrogen-doped graphene aerogel for enhanced visible-light photocatalytic pollutant degradation and hydrogen evolution. *RSC Adv.* **2020,** *10*, 12423-12431, https://doi.org/10.1039/D0RA01630F.
92. Zhong, Y.; Mahmud, S.; He, Z.; Yang, Y.; Zhang, Z.; Guo, F.; Chen, Z.; Xiong, Z.; Zhao, Y. Graphene oxide modified membrane for highly efficient wastewater treatment by dynamic combination of nanofiltration and catalysis. *J. Hazard. Mater.* **2020,** *397*, 122774, https://doi.org/10.1016/j.jhazmat.2020.122774.
93. Zhang, J.-Y.; Zhang, S.-H.; Li, J.; Zheng, X.-C.; Guan, X.-X. Constructing of 3D graphene aerogel-g-C3N4 metal-free heterojunctions with superior purification efficiency for organic dyes. *J. Mol. Liq.* **2020,** *310*, 113242, https://doi.org/10.1016/j.molliq.2020.113242.
94. Ussia, M.; Ruffino, F.; Bruno, E.; Spina, E.; Conticello, I.; Privitera, V.; Carroccio, S. C. The role of solvent on the formulation of graphene/polyporphyrin hybrid material versus photocatalytic activity. *Polym. Bull.* **2020,** *77*, 2073-2087, https://doi.org/10.1007/s00289-019-02849-1.
95. Sandhu, I. S.; Chitkara, M.; Rana, S.; Dhillon, G.; Taneja, A.; Kumar, S. Photocatalytic performances of stand-alone graphene oxide (GO) and reduced graphene oxide (rGO) nanostructures. *Opt. Quant. Electron.* **2020,** *52*, 1-16, https://doi.org/10.1007/s11082-020-02473-8.
96. Liu, J.; Bai, H.; Wang, Y.; Liu, Z.; Zhang, X.; Sun, D. D. Self-assembling TiO2 nanorods on large graphene oxide sheets at a two-phase interface and their anti-recombination in photocatalytic applications. *Adv. Funct. Mater.* **2010,** *20* , 4175-4181, https://doi.org/10.1002/adfm.201001391.
97. Chen, W.; Ye, T.; Xu, H.; Chen, T.; Geng, N.; Gao, X. An ultrafiltration membrane with enhanced photocatalytic performance from grafted N–TiO 2/graphene oxide. *RSC Adv.* **2017,** *7*, 9880-9887, https://doi.org/10.1039/C6RA27666K.
98. Hua, Y.; Wang, S.; Xiao, J.; Cui, C.; Wang, C. Preparation and characterization of Fe 3 O 4/gallic acid/graphene oxide magnetic nanocomposites as highly efficient Fenton catalysts. *RSC Adv.* **2017,** *7*, 28979-28986, https://doi.org/10.1039/C6RA23939K.
99. Wang, M.; Cai, L.; Jin, Q.; Zhang, H.; Fang, S.; Qu, X.; Zhang, Z.; Zhang, Q. One-pot composite synthesis of three-dimensional graphene oxide/poly (vinyl alcohol)/TiO2 microspheres for organic dye removal. *Sep. Purif. Technol.* **2017,** *172*, 217-226, https://doi.org/10.1016/j.seppur.2016.08.015.
100. Fu, X.; Zhan, Y.; Meng, Y.; Li, Y.; Liao, C.; Lu, Z. Graphene oxide/poly (vinyl alcohol) hydrogels with good tensile properties and reusable adsorption properties. *Plast Rubber Compos.* **2017,** *46*, 53-59, https://doi.org/10.1080/14658011.2016.1268755.

101. Atchudan, R.; Edison, T. N. J. I.; Perumal, S.; Karthikeyan, D.; Lee, Y. R. Effective photocatalytic degradation of anthropogenic dyes using graphene oxide grafting titanium dioxide nanoparticles under UV-light irradiation. *J. Photochem. Photobiol. A Chem.* **2017,** *333*, 92-104, https://doi.org/10.1016/j.jphotochem.2016.10.021.
102. Pruna, A.; Shao, Q.; Kamruzzaman, M.; Li, Y.; Zapien, J.; Pullini, D.; Mataix, D. B.; Ruotolo, A. Effect of ZnO core electrodeposition conditions on electrochemical and photocatalytic properties of polypyrrole-graphene oxide shelled nanoarrays. *Appl. Surf. Sci.* **2017,** *392*, 801-809, https://doi.org/10.1016/j.apsusc.2016.09.122.
103. Wan, Y.; Liang, C.; Xia, Y.; Huang, W.; Li, Z. Fabrication of graphene oxide enwrapped Z-scheme Ag2SO3/AgBr nanoparticles with enhanced visible-light photocatalysis. *Appl. Surf. Sci.* **2017,** *396*, 48-57, https://doi.org/10.1016/j.apsusc.2016.10.189.
104. Atchudan, R.; Edison, T. N. J. I.; Perumal, S.; Shanmugam, M.; Lee, Y. R. Direct solvothermal synthesis of zinc oxide nanoparticle decorated graphene oxide nanocomposite for efficient photodegradation of azo-dyes. *J. Photochem. Photobiol. A Chem.* **2017,** *337*, 100-111, https://doi.org/10.1016/j.jphotochem.2017.01.021.
105. Granbohm, H.; Kulmala, K.; Iyer, A.; Ge, Y.; Hannula, S.-P. Preparation and photocatalytic activity of quaternary GO/TiO 2/Ag/AgCl nanocomposites. *Water Air Soil Pollut.* **2017,** *228*, 127, https://doi.org/10.1007/s11270-017-3313-9. .
106. Ali, I.; Kim, S.-R.; Park, K.; Kim, J.-O. One-step electrochemical synthesis of graphene oxide-TiO 2 nanotubes for improved visible light activity. *Opt. Mater. Express* **2017,** *7*, 1535-1546, https://doi.org/10.1364/OME.7.001535.
107. Liu, Y.; Jin, W.; Zhao, Y.; Zhang, G.; Zhang, W. Enhanced catalytic degradation of methylene blue by α-Fe2O3/graphene oxide via heterogeneous photo-Fenton reactions. *Appl. Catal. B. Environ.* **2017,** *206*, 642-652, https://doi.org/10.1016/j.apcatb.2017.01.075.
108. Omidvar, A.; Jaleh, B.; Nasrollahzadeh, M., Preparation of the GO/Pd nanocomposite and its application for the degradation of organic dyes in water. *J. Colloid Interface Sci.* **2017,** *496*, 44-50, https://doi.org/10.1016/j.jcis.2017.01.113.
109. Yu, Y.; Yang, Q.; Yu, X.; Lu, Q.; Hong, X. Highly Efficient Metal-Free Visible Light Driven Photocatalyst: Graphene Oxide/Polythiophene Composite. *ChemistrySelect* **2017,** *2*, 5578-5586, https://doi.org/10.1002/slct.201700974.
110. Chen, F.; Yang, Q.; Wang, S.; Yao, F.; Sun, J.; Wang, Y.; Zhang, C.; Li, X.; Niu, C.; Wang, D. Graphene oxide and carbon nitride nanosheets co-modified silver chromate nanoparticles with enhanced visible-light photoactivity and anti-photocorrosion properties towards multiple refractory pollutants degradation. *Appl. Catal. B. Environ.* **2017,** *209*, 493-505, https://doi.org/10.1016/j.apcatb.2017.03.026.
111. Ravichandran, K.; Uma, R.; Sriram, S.; Balamurgan, D. Fabrication of ZnO: Ag/GO composite thin films for enhanced photocatalytic activity. *Ceramics Int.* **2017,** *43*, 10041-1005, https://doi.org/10.1016/j.ceramint.2017.05.020.
112. Liu, Y.; Liu, X.; Zhao, Y.; Dionysiou, D. D. Aligned α-FeOOH nanorods anchored on a graphene oxide-carbon nanotubes aerogel can serve as an effective Fenton-like oxidation catalyst. *Appl. Catal. B. Environ.* **2017,** *213*, 74-86, https://doi.org/10.1016/j.apcatb.2017.05.019.
113. Zhu, C.; Liu, G.; Han, K.; Ye, H.; Wei, S.; Zhou, Y. One-step facile synthesis of graphene oxide/TiO2 composite as efficient photocatalytic membrane for water treatment: Crossflow filtration operation and membrane fouling analysis. *Chem. Eng. Process.* **2017,** *120*, 20-26, https://doi.org/10.1016/j.cep.2017.06.012.
114. Kumar, A.; Rout, L.; Achary, L. S. K.; Mohanty, S. K.; Dash, P. A combustion synthesis route for magnetically separable graphene oxide–CuFe 2 O 4–ZnO nanocomposites with enhanced solar light-mediated photocatalytic activity. *New J. Chem.* **2017,** *41*, 10568-10583, https://doi.org/10.1039/C7NJ02070H.
115. Liu, Y.; Yang, D.; Yu, R.; Qu, J.; Shi, Y.; Li, H.; Yu, Z.-Z. Tetrahedral silver phosphate/graphene oxide hybrids as highly efficient visible light photocatalysts with excellent cyclic stability. *J. Phys. Chem. C* **2017,** *121*, 25172-25179, https://doi.org/10.1021/acs.jpcc.7b07848.
116. Yilmaz, E.; Soylak, M. Facile and green solvothermal synthesis of palladium nanoparticle-nanodiamond-graphene oxide material with improved bifunctional catalytic properties. *J. Iran. Chem. Soc.* **2017,** *14*, 2503-2512, https://doi.org/10.1007/s13738-017-1185-y.

117. Channei, D.; Nakaruk, A.; Phanichphant, S. Influence of graphene oxide on photocatalytic enhancement of cerium dioxide. *Mat. Lett.* **2017,** *209*, 43-47, https://doi.org/10.1016/j.matlet.2017.07.109.
118. Miao, X.; Yue, X.; Shen, X.; Ji, Z.; Zhou, H.; Zhu, G.; Wang, J.; Kong, L.; Liu, M.; Song, C. Nitrogen-doped carbon dot-modified Ag 3 PO 4/GO photocatalyst with excellent visible-light-driven photocatalytic performance and mechanism insight. *Catal. Sci. Technol.* **2018,** *8*, 632-641, https://doi.org/10.1039/C7CY01883E.
119. Tanhaei, M.; Mahjoub, A. R.; Safarifard, V. Sonochemical synthesis of amide-functionalized metal-organic framework/graphene oxide nanocomposite for the adsorption of methylene blue from aqueous solution. *Ultrason. Sonochem.* **2018,** *41*, 189-195, https://doi.org/10.1016/j.ultsonch.2017.09.030.
120. Ahmad, J.; Majid, K. Enhanced visible light driven photocatalytic activity of CdO–graphene oxide heterostructures for the degradation of organic pollutants. *New J. Chem.* **2018,** *42*, 3246-3259, https://doi.org/10.1039/C7NJ03617E.
121. Molla, A.; Li, Y.; Khandelwal, M.; Mandal, B.; Kang, S. G.; Hur, S. H.; Chung, J. S. Facile synthesis and structural analysis of graphene oxide decorated with iron-cerium carbonate for visible-light driven rapid degradation of organic dyes. *J. Environ. Chem. Eng.* **2018,** *6*, 2616-2626, https://doi.org/10.1016/j.jece.2018.04.007.
122. Wang, H.; Shen, Q.; You, Z.; Su, Y.; Yu, Y.; Babapour, A.; Zhang, F.; Cheng, D.; Yang, H. Preparation of nanoscale-dispersed g-C3N4/graphene oxide composite photocatalyst with enhanced visible-light photocatalytic activity. *Mat. Lett.* **2018,** *217*, 143-145, https://doi.org/10.1016/j.matlet.2018.01.037.
123. Zhou, H.; Yue, X.; Lv, H.; Kong, L.; Ji, Z.; Shen, X. Graphene oxide-FePO4 nanocomposite: Synthesis, characterization and photocatalytic properties as a Fenton-like catalyst. *Ceramics Int.* **2018,** *44*, 7240-7244, https://doi.org/10.1016/j.ceramint.2018.01.176.
124. Jeevitha, G.; Abhinayaa, R.; Mangalaraj, D.; Ponpandian, N. Tungsten oxide-graphene oxide (WO3-GO) nanocomposite as an efficient photocatalyst, antibacterial and anticancer agent. *J. Phys. Chem. Solids* **2018,** *116*, 137-147, https://doi.org/10.1016/j.jpcs.2018.01.021.
125. Soleimani, K.; Tehrani, A. D.; Adeli, M. Preparation of new GO-based slide ring hydrogel through a convenient one-pot approach as methylene blue absorbent. *Carbohydr. Polym.* **2018,** *187*, 94-101, https://doi.org/10.1016/j.carbpol.2018.01.084.
126. Pruna, A.; Wu, Z.; Zapien, J.; Li, Y.; Ruotolo, A. Enhanced photocatalytic performance of ZnO nanostructures by electrochemical hybridization with graphene oxide. *Appl. Surf. Sci.* **2018,** *441*, 936-944, https://doi.org/10.1016/j.apsusc.2018.02.117.
127. Wan, J.; An, B.; Chen, Z.; Zhang, J.; William, W. Y. Nitrogen doped graphene oxide modified WSe2 nanorods for visible light photocatalysis. *J. Alloys Comp.* **2018,** *750*, 499-506, https://doi.org/10.1016/j.jallcom.2018.04.047.
128. Molla, A.; Li, Y.; Khandelwal, M.; Hur, S. H.; Chung, J. S. Anion-controlled sulfidation for decoration of graphene oxide with iron cobalt sulfide for rapid sonochemical dyes removal in the absence of light. *Appl. Catal. A. Gen.* **2018,** *561*, 49-58, https://doi.org/10.1016/j.apcata.2018.05.014.
129. Choi, B.-K.; Choi, W.-K.; Park, S.-J.; Seo, M.-K. One-pot synthesis of Ag-TiO2/nitrogen-doped graphene oxide nanocomposites and its photocatalytic degradation of methylene blue. *J. Nanosci. Nanotechnol.* **2018,** *18*, 6075-6080, https://doi.org/10.1166/jnn.2018.15616.
130. Zhao, Y.; Zhang, X.; Liu, J.; Wang, C.; Li, J.; Jin, H. Graphene oxide modified nano-sized BaTiO3 as photocatalyst. *Ceramics Int.* **2018,** *44*, 15929-15934, https://doi.org/10.1016/j.ceramint.2018.06.013.
131. Li, L.; Xue, S.; Xie, P.; Feng, H.; Hou, X.; Liu, Z.; Xu, Z.; Zou, R. Facile synthesis and characterization of GO/ZnS nanocomposite with highly efficient photocatalytic activity. *Electron. Mater. Lett.* **2018,** *14*, 739-748, https://doi.org/10.1007/s13391-018-0082-6.
132. Zarrabi, M.; Haghighi, M.; Alizadeh, R. Sonoprecipitation dispersion of ZnO nanoparticles over graphene oxide used in photocatalytic degradation of methylene blue in aqueous solution: influence of irradiation time and power. *Ultrason. Sonochem.* **2018,** *48*, 370-382, https://doi.org/10.1016/j.ultsonch.2018.05.034.
133. Ahmad, J.; Majid, K.; Dar, M. A. Controlled synthesis of p-type NiO/n-type GO nanocomposite with enhanced photocatalytic activity and study of temperature effect on the photocatalytic activity of the nanocomposite. *Appl. Surf. Sci.* **2018,** *457*, 417-426, https://doi.org/10.1016/j.apsusc.2018.06.200.
134. Zhang, D.; Zhao, Y.; Chen, L. Fabrication and characterization of amino-grafted graphene oxide modified ZnO with high photocatalytic activity. *Appl. Surf. Sci.* **2018,** *458*, 638-647, https://doi.org/10.1016/j.apsusc.2018.07.053.

135. Wang, X.; Zhou, B.; Zhang, Y.; Liu, L.; Song, J.; Hu, R.; Qu, J. In-situ reduction and deposition of Ag nanoparticles on black phosphorus nanosheets co-loaded with graphene oxide as a broad spectrum photocatalyst for enhanced photocatalytic performance. *J. Alloys Comp.* **2018,** *769*, 316-324, https://doi.org/10.1016/j.jallcom.2018.08.008.
136. Ahmad, J.; Sofi, F. A.; Mehraj, O.; Majid, K. Fabrication of highly photocatalytic active anatase TiO2-graphene oxide heterostructures via solid phase ball milling for environmental remediation. *Surf. Interfaces* **2018,** *13*, 186-195, https://doi.org/10.1016/j.surfin.2018.09.010.
137. Datcu, A.; Mendoza, M.; del Pino, A. P.; Logofatu, C.; Luculescu, C.; György, E. UV–vis light induced photocatalytic activity of TiO2/graphene oxide nanocomposite coatings. *Catal. Today* **2019,** *321*, 81-86, https://doi.org/10.1016/j.cattod.2018.02.026.
138. Mohamed, M. M.; Bayoumy, W.; El-Ashkar, T. M.; Goher, M.; Abdo, M. Graphene oxide dispersed in N-TiO2 nanoplatelets and their implication in wastewater remediation under visible light illumination: Photoelectrocatalytic and photocatalytic properties. *J. Environ. Chem. Eng.* **2019,** *7*, 102884, https://doi.org/10.1016/j.jece.2019.102884.
139. Zhang, D.; Dai, F.; Zhang, P.; An, Z.; Zhao, Y.; Chen, L. The photodegradation of methylene blue in water with PVDF/GO/ZnO composite membrane. *Mater. Sci. Eng. C* **2019,** *96*, 684-692, https://doi.org/10.1016/j.msec.2018.11.049.
140. Das, R. S.; Warkhade, S. K.; Kumar, A.; Wankhade, A. V. Graphene oxide-based zirconium oxide nanocomposite for enhanced visible light-driven photocatalytic activity. *Res. Chem. Intermed.* **2019,** *45*, 1689-1705, https://doi.org/10.1007/s11164-018-3699-z.
141. Kaur, J.; Kaur, M. Facile fabrication of ternary nanocomposite of MgFe2O4 TiO2@ GO for synergistic adsorption and photocatalytic degradation studies. *Ceramics Int.* **2019,** *45*, 8646-8659, https://doi.org/10.1016/j.ceramint.2019.01.185.
142. Xu, T.; Lei, X.; Gu, G.; Zou, R.; Wu, Q. Facile synthesis of CeO2-graphene oxide composites with enhanced visible-light photocatalytic performance. *Mater. Sci. Eng. B* **2019,** *244*, 49-55, https://doi.org/10.1016/j.mseb.2019.04.023.
143. Janani, R.; Menon, S. S.; Bhalerao, G.; Gupta, B.; Singh, S. Zn1-xGaxO1-yNy–Graphene oxide nanocomposite for enhanced visible–Light photocatalytic activity. *Dyes Pigm.* **2019,** *165*, 249-255, https://doi.org/10.1016/j.dyepig.2019.02.020.
144. Mohamed, H. H. Rationally designed Fe2O3/GO/WO3 Z-Scheme photocatalyst for enhanced solar light photocatalytic water remediation. *J. Photochem. Photobiol. A Chem.* **2019,** *378*, 74-84, https://doi.org/10.1016/j.jphotochem.2019.04.023.
145. He, Y. W.; Wang, Q.; Yan, X.; He, L. Q.; Zhang, G. Q.; Li, X. L. Ultrafast degradation of common organic dyes in presence of gadolinium oxide/graphene oxide in water. *Fuller. Nanotub. Car. N.* **2019,** *27*, 478-481, https://doi.org/10.1080/1536383X.2019.1592162.
146. Singh, M.; Singh, J.; Rawat, M.; Sharma, J.; Singh, P. P. Enhanced photocatalytic degradation of hazardous industrial pollutants with inorganic–organic TiO 2–SnO 2–GO hybrid nanocomposites. *J. Mater. Sci.: Mater. Electron.* **2019,** *30*, 13389-13400, https://doi.org/10.1007/s10854-019-01706-1.
147. Naz, S.; Mansoor, Q.; Nisar, A.; Karim, S.; Khan, M.; Ali, G.; Rahman, A.; Ahmad, M. Silver nanoparticles embedded graphene oxide nanocomposite with enhanced antibacterial and photocatalytic degradation activities. *ChemistrySelect* **2019,** *4* , 8372-8377, https://doi.org/10.1002/slct.201901124.
148. Abdel-Mottaleb, M.; Khalil, A.; Karim, S.; Osman, T.; Khattab, A. High performance of PAN/GO-ZnO composite nanofibers for photocatalytic degradation under visible irradiation. *J. Mech. Behav. Biomed. Mater.* **2019,** *96*, 118-124, https://doi.org/10.1016/j.jmbbm.2019.04.040.
149. Neto, N. A.; Oliveira, Y.; Nascimento, J.; Carvalho, B.; Bomio, M.; Motta, F. Synthesis, characterization, optical properties investigation and reusability photocatalyst capacity of AgCl-xGO composite. *J. Mater. Sci.: Mater. Electron.* **2019,** *30*, 15214-15223, https://doi.org/10.1007/s10854-019-01894-w.
150. Esmaeili, N.; Mohammadi, P.; Abbaszadeh, M.; Sheibani, H. Au nanoparticles decorated on magnetic nanocomposite (GO-Fe3O4/Dop/Au) as a recoverable catalyst for degradation of methylene blue and methyl orange in water. *Int. J. Hydrog. Energy* **2019,** *44*, 23002-23009, https://doi.org/10.1016/j.ijhydene.2019.07.025.
151. Mohamed, M. M.; Ghanem, M. A.; Khairy, M.; Naguib, E.; Alotaibi, N. H. Zinc oxide incorporated carbon nanotubes or graphene oxide nanohybrids for enhanced sonophotocatalytic degradation of methylene blue dye. *Appl. Surf. Sci.* **2019,** *487*, 539-549, https://doi.org/10.1016/j.apsusc.2019.05.135.

152. Xiao, F.; Ren, H.; Zhou, H.; Wang, H.; Wang, N.; Pan, D. Porous montmorillonite@ graphene oxide@ Au nanoparticle composite microspheres for organic dye degradation. *ACS Appl. Nano Mater.* **2019,** *2*, 5420-5429, https://doi.org/10.1021/acsanm.9b01043.
153. Sobhani-Nasab, A.; Behvandi, S.; Karimi, M. A.; Sohouli, E.; Karimi, M. S.; Gholipour, N.; Ahmadi, F.; Rahimi-Nasrabadi, M. Synergetic effect of graphene oxide and C3N4 as co-catalyst for enhanced photocatalytic performance of dyes on Yb2 (MoO4) 3/YbMoO4 nanocomposite. *Ceramics Int.* **2019,** *45*, 17847-17858, https://doi.org/10.1016/j.ceramint.2019.05.356.
154. Liu, Y.; Yin, H.; Xu, C.; Zhuge, X.; Wan, J. Polythiophene-tungsten selenide/nitrogen-doped graphene oxide nanocomposite for visible light-driven photocatalysis. *J. Nanoparticle Res.* **2019,** *21*, 1-13, https://doi.org/10.1007/s11051-019-4648-5.
155. Khan, S. A.; Arshad, Z.; Shahid, S.; Arshad, I.; Rizwan, K.; Sher, M.; Fatima, U. Synthesis of TiO2/Graphene oxide nanocomposites for their enhanced photocatalytic activity against methylene blue dye and ciprofloxacin. *Compos. B. Eng.* **2019,** *175*, 107120, https://doi.org/10.1016/j.compositesb.2019.107120.
156. Muthukumaran, M.; Dhinagaran, G.; Narayanan, V.; Raju, T.; Venkatachalam, K.; Karthika, P.; Vivekananthandan, S.; Sagadevan, S.; Roselin, L. S.; Selvin, R. Enhanced photocatalytic behavior of (GO/Cu2O) composite with Cu2O being synthesized through green route. *J. Nanosci. Nanotechnol.* **2019,** *19*, 7215-7220, https://doi.org/10.1166/jnn.2019.16671.
157. Nie, J.; Li, C.-y.; Jin, Z.-y.; Hu, W.-t.; Wang, J.-h.; Huang, T.; Wang, Y. Fabrication of MCC/Cu2O/GO composite foam with high photocatalytic degradation ability toward methylene blue. *Carbohydr. Polym.* **2019,** *223*, 115101, https://doi.org/10.1016/j.carbpol.2019.115101.
158. Qi, Z.; Wang, K.; Jiang, Y.; Zhu, Y.; Chen, X.; Tang, Q.; Ren, Y.; Zheng, C.; Gao, D.; Wang, C. Preparation and characterization of SnO 2− x/GO composite photocatalyst and its visible light photocatalytic activity for self-cleaning cotton fabrics. *Cellulose* **2019,** *26*, 8919-8937, https://doi.org/10.1007/s10570-019-02662-z.
159. Song, S.; Wang, Y.; Shen, H.; Zhang, J.; Mo, H.; Xie, J.; Zhou, N.; Shen, J. Ultrasmall graphene oxide modified with Fe3O4 nanoparticles as a Fenton-like agent for methylene blue degradation. *ACS Appl. Nano Mater.* **2019,** *2*, 7074-7084, https://doi.org/10.1021/acsanm.9b01608.
160. Kaur, K.; Jindal, R. Self-assembled GO incorporated CMC and Chitosan-based nanocomposites in the removal of cationic dyes. *Carbohydr. Polym.* **2019,** *225*, 115245, https://doi.org/10.1016/j.carbpol.2019.115245.
161. Nejad, M. S.; Seyedi, N.; Sheibani, H. Fabrication of functionalized two dimensional graphene oxide and promoted with phosphotungstic acid for reduction of organic dyes in water. *Mater. Chem. Phys.* **2019,** *238*, 121849, https://doi.org/10.1016/j.matchemphys.2019.121849.
162. Ramos-Corona, A.; Rangel, R.; Alvarado-Gil, J.; Bartolo-Pérez, P.; Quintana, P.; Rodríguez-Gattorno, G. Photocatalytic performance of nitrogen doped ZnO structures supported on graphene oxide for MB degradation. *Chemosphere* **2019,** *236*, 124368, https://doi.org/10.1016/j.chemosphere.2019.124368.
163. Mengting, Z.; Kurniawan, T. A.; Fei, S.; Ouyang, T.; Othman, M. H. D.; Rezakazemi, M.; Shirazian, S. Applicability of BaTiO3/graphene oxide (GO) composite for enhanced photodegradation of methylene blue (MB) in synthetic wastewater under UV–vis irradiation. *Environ. Pollut.* **2019,** *255*, 113182, https://doi.org/10.1016/j.envpol.2019.113182.
164. Wang, R.; Shi, K.; Huang, D.; Zhang, J.; An, S. Synthesis and degradation kinetics of TiO 2/GO composites with highly efficient activity for adsorption and photocatalytic degradation of MB. *Sci. Rep.* **2019,** *9*, 1-9, https://doi.org/10.1038/s41598-019-54320-w.
165. Nas, M. S.; Calimli, M. H.; Burhan, H.; Yılmaz, M.; Mustafov, S. D.; Sen, F. Synthesis, characterization, kinetics and adsorption properties of Pt-Co@ GO nano-adsorbent for methylene blue removal in the aquatic mediums using ultrasonic process systems. *J. Mol. Liq.* **2019,** *296*, 112100, https://doi.org/10.1016/j.molliq.2019.112100.
166. Ashraf, M. A.; Li, C.; Zhang, D.; Fakhri, A. Graphene oxides as support for the synthesis of nickel sulfide–indium oxide nanocomposites for photocatalytic, antibacterial and antioxidant performances. *Appl. Organomet. Chem.* **2020,** *34*, e5354, https://doi.org/10.1002/aoc.5354.
167. Xu, B.; Maimaiti, H.; Wang, S.; Awati, A.; Wang, Y.; Zhang, J.; Chen, T. Preparation of coal-based graphene oxide/SiO2 nanosheet and loading ZnO nanorod for photocatalytic Fenton-like reaction. *Appl. Surf. Sci.* **2019,** *498*, 143835, https://doi.org/10.1016/j.apsusc.2019.143835.

168. Maruthupandy, M.; Qin, P.; Muneeswaran, T.; Rajivgandhi, G.; Quero, F.; Song, J.-M. Graphene-zinc oxide nanocomposites (G-ZnO NCs): Synthesis, characterization and their photocatalytic degradation of dye molecules. *Mater. Sci. Eng. B*, **2020,** *254*, 114516, https://doi.org/10.1016/j.mseb.2020.114516.
169. Xia, Y.-M.; Zhang, J.-H.; Xia, M.; Zhao, Y.; Chu, S.-P.; Gao, W.-W. Peony-like magnetic graphene oxide/Fe 3 O 4/BiOI nanoflower as a novel photocatalyst for enhanced photocatalytic degradation of Rhodamine B and Methylene blue dyes. *J. Mater. Sci.: Mater. Electron.* **2020,** *31*, 1996-2009, https://doi.org/10.1007/s10854-019-02719-6.
170. Avramescu, S.; Petrescu, S.; Culita, D. C.; Tudose, M.; Hanganu, A.; Zarafu, I.; Ionita, P. A mixed organic functionalized silica-graphene oxide as advanced material for pollutant removal. *J. Nanoparticle Res.* **2020,** *22*, 1-9, https://doi.org/10.1007/s11051-020-04935-2.
171. Bayantong, A. R. B.; Shih, Y.-J.; Dong, C.-D.; Garcia-Segura, S.; de Luna, M. D. G. Nickel ferrite nanoenabled graphene oxide (NiFe 2 O 4@ GO) as photoactive nanocomposites for water treatment. *Environ. Sci. Pollut. Res.* **2021,** *28*, 5472-5481, https://doi.org/10.1007/s11356-020-10545-1.
172. Trinh, D. T. T.; Channei, D.; Chansaenpak, K.; Khanitchaidecha, W.; Nakaruk, A. Photocatalytic degradation of organic dye over bismuth vanadate–silicon dioxide–graphene oxide nanocomposite under visible light irradiation. *J. Aust. Ceram. Soc.* **2020**, *56*, 1237-1241, https://doi.org/10.1007/s41779-020-00470-4.
173. Tara, N.; Siddiqui, S. I.; Nirala, R. K.; Abdulla, N. K.; Chaudhry, S. A. Synthesis of antibacterial, antioxidant and magnetic Nigella sativa-graphene oxide based nanocomposite BC-GO@ Fe3O4 for water treatment. *Colloids Interface Sci. Commun.* **2020,** *37*, 100281, https://doi.org/10.1016/j.colcom.2020.100281.
174. Kurniawan, T. A.; Mengting, Z.; Fu, D.; Yeap, S. K.; Othman, M. H. D.; Avtar, R.; Ouyang, T. Functionalizing TiO2 with graphene oxide for enhancing photocatalytic degradation of methylene blue (MB) in contaminated wastewater. *J. Environ. Manage.* **2020,** *270*, 110871, https://doi.org/10.1016/j.jenvman.2020.110871.
175. Al-Wafi, R.; Ahmed, M.; Mansour, S. Tuning the synthetic conditions of graphene oxide/magnetite/hydroxyapatite/cellulose acetate nanofibrous membranes for removing Cr (VI), Se (IV) and methylene blue from aqueous solutions. *J. Water Process Eng.* **2020,** *38*, 101543, https://doi.org/10.1016/j.jwpe.2020.101543.
176. Liu, Y.; Li, K.; Xu, W.; Du, B.; Wei, Q.; Liu, B.; Wei, D. GO/PEDOT: NaPSS modified cathode as heterogeneous electro-Fenton pretreatment and subsequently aerobic granular sludge biological degradation for dye wastewater treatment. *Sci. Total Environ.* **2020,** *700*, 134536, https://doi.org/10.1016/j.scitotenv.2019.134536.
177. Bai, Y.; Zhang, S.; Feng, S.; Zhu, M.; Ma, S. The first ternary Nd-MOF/GO/Fe 3 O 4 nanocomposite exhibiting an excellent photocatalytic performance for dye degradation. *Dalton Trans.* **2020,** *49*, 10745-10754, https://doi.org/10.1039/D0DT01648A.
178. Chen, Y.; Xiang, Z.; Wang, D.; Kang, J.; Qi, H. Effective photocatalytic degradation and physical adsorption of methylene blue using cellulose/GO/TiO 2 hydrogels. *RSC Adv.* **2020,** *10*, 23936-23943, https://doi.org/10.1039/D0RA04509H.
179. Ahmed, M.; El-Naggar, M. E.; Aldalbahi, A.; El-Newehy, M. H.; Menazea, A. Methylene blue degradation under visible light of metallic nanoparticles scattered into graphene oxide using laser ablation technique in aqueous solutions. *J. Mol. Liq.* **2020,** *315*, 113794, https://doi.org/10.1016/j.molliq.2020.113794.
180. Akshatha, S.; Sreenivasa, S.; Kumar, K. Y.; Archana, S.; Prashanth, M.; Prasanna, B.; Chakraborty, P.; Krishnaiah, P.; Raghu, M.; Alrobei, H. Rutile, mesoporous ruthenium oxide decorated graphene oxide as an efficient visible light driven photocatalyst for hydrogen evolution reaction and organic pollutant degradation. *Mater. Sci. Semicond. Process.* **2020,** *116*, 105156, https://doi.org/10.1016/j.mssp.2020.105156. .
181. Arunpandian, M.; Selvakumar, K.; Raja, A.; Rajasekaran, P.; Ramalingan, C.; Nagarajan, E.; Pandikumar, A.; Arunachalam, S. Rational design of novel ternary Sm2WO6/ZnO/GO nanocomposites: An affordable photocatalyst for the mitigation of carcinogenic organic pollutants. *Colloids Surf. A Physicochem. Eng. Asp.* **2020,** *596*, 124721, https://doi.org/10.1016/j.colsurfa.2020.124721.
182. Behvandi, S.; Sobhani-Nasab, A.; Karimi, M. A.; Sohouli, E.; Karimi, M.; Ganjali, M. R.; Ahmadi, F.; Rahimi-Nasrabadi, M. Synthesis and characterization of Sm2 (MoO4) 3, Sm2 (MoO4) 3/GO and Sm2 (MoO4) 3/C3N4 nanostructures for improved photocatalytic performance and their anti-cancer the MCF-7 cells. *Polyhedron* **2020,** *180*, 114424, https://doi.org/10.1016/j.poly.2020.114424.

183. Biswas, M. R. U. D.; Ho, B. S.; Oh, W.-C. Eco-friendly conductive polymer-based nanocomposites, BiVO 4/graphene oxide/polyaniline for excellent photocatalytic performance. *Polym. Bull.* **2020,** *77*, 4381-4400, https://doi.org/10.1007/s00289-019-02973-y.
184. Gupta, A.; Viltres, H.; Gupta, N. K. Sono-adsorption of organic dyes onto CoFe2O4/Graphene oxide nanocomposite. *Surf. Interfaces* **2020,** *20*, 100563, https://doi.org/10.1016/j.surfin.2020.100563.
185. Hasan, J.; Li, H.; Tian, G.; Qin, C. Fabrication of Cr2S3-GO-TiO2 composite with high visible-light-driven photocatalytic activity on degradation of organic dyes. *Chem. Phys.* **2020,** *539*, 110950, https://doi.org/10.1016/j.chemphys.2020.110950.
186. Kaushal, S.; Kaur, N.; Kaur, M.; Singh, P. P. Dual-Responsive Pectin/Graphene Oxide (Pc/GO) nano-composite as an efficient adsorbent for Cr (III) ions and photocatalyst for degradation of organic dyes in waste water. *J. Photochem. Photobiol. A Chem.* **2020,** *403*, 112841, https://doi.org/10.1016/j.jphotochem.2020.112841.
187. Qureshi, I.; Khan, S.; Shifa, M. S.; Wazir, A. H. Graphene oxide-based ZnFe2O4 catalyst for efficient adsorption and degradation of methylene blue from water. *J. Disper. Sci. Technol.* **2020**, 1-7, https://doi.org/10.1080/01932691.2020.1839483.
188. Samuel, M. S.; Suman, S.; Selvarajan, E.; Mathimani, T.; Pugazhendhi, A. Immobilization of Cu3 (btc) 2 on graphene oxide-chitosan hybrid composite for the adsorption and photocatalytic degradation of methylene blue. *J. Photochem. Photobiol. B Biol.* **2020,** *204*, 111809, https://doi.org/10.1016/j.jphotobiol.2020.111809.
189. Gettler, A. O.; Sunshine, I. Colorimetric determination of alkaloids in tissues by means of methyl orange. *Anal. Chem.* **1951,** *23*, 779-781, https://doi.org/10.1021/ac60053a028.
190. Tong, Z.; Yang, D.; Shi, J.; Nan, Y.; Sun, Y.; Jiang, Z. Three-dimensional porous aerogel constructed by g-C3N4 and graphene oxide nanosheets with excellent visible-light photocatalytic performance. *ACS Appl. Mater. Interfaces* **2015,** *7*, 25693-25701, https://doi.org/10.1021/acsami.5b09503.
191. Gong, J.; Gao, X.; Li, M.; Nie, Q.; Pan, W.; Liu, R. Dye adsorption on electrochemical exfoliated graphene oxide nanosheets: pH influence, kinetics and equilibrium in aqueous solution. *Int. J. Environ. Sci. Technol.* **2017,** *14*, 305-314, https://doi.org/10.1007/s13762-016-1143-8.
192. Peng, W.; Li, X. Synthesis of a sulfur-graphene composite as an enhanced metal-free photocatalyst. *Nano Res.* **2013,** *6*, 286-292, https://doi.org/10.1007/s12274-013-0306-x.
193. Xu, H.-M.; Sun, X.-F.; Wang, S.-Y.; Song, C.; Wang, S.-G. Development of laccase/graphene oxide membrane for enhanced synthetic dyes separation and degradation. *Sep. Purif. Technol.* **2018,** *204*, 255-260, https://doi.org/10.1016/j.seppur.2018.04.036.
194. Wu, S.; Wen, S.; Xu, X.; Huang, G.; Cui, Y.; Li, J.; Qu, A. Facile synthesis of porous graphene-like carbon nitride nanosheets with high surface area and enhanced photocatalytic activity via one-step catalyst-free solution self-polymerization. *Appl. Surf. Sci.* **2018,** *436*, 424-432, https://doi.org/10.1016/j.apsusc.2017.11.254.
195. Vellaichamy, B.; Paulmony, T. Visible light active metal-free photocatalysis: N-doped graphene covalently grafted with g-C3N4 for highly robust degradation of methyl orange. *Solid State Sci.* **2019,** *94*, 99-105, https://doi.org/10.1016/j.solidstatesciences.2019.06.003.
196. Molla, A.; Li, Y.; Mandal, B.; Kang, S. G.; Hur, S. H.; Chung, J. S. Selective adsorption of organic dyes on graphene oxide: theoretical and experimental analysis. *Appl. Surf. Sci.* **2019,** *464*, 170-177, https://doi.org/10.1016/j.apsusc.2018.09.056.
197. Wang, F. Preparation of N-Doped Graphene and Its Performance in Degradation of Methyl Orange. *Russ. J. Phys. Chem. A* **2019,** *93*, 2263-2268, https://doi.org/10.1134/S0036024419110347.
198. Labiadh, L.; Kamali, A. R. Textural, structural and morphological evolution of mesoporous 3D graphene saturated with methyl orange dye during thermal regeneration. *Diam. Relat. Mater.* **2020,** *103*, 107698, https://doi.org/10.1016/j.diamond.2020.107698.
199. Song, Y.-h.; Xu, Q.-t.; He, T.; Wang, Z.-y.; Yu, L. Efficient biodegradation of azo dyes catalyzed by the anthraquinone-2-sulfonate and reduced graphene oxide nanocomposite. *ACS Omega* **2020,** *5*, 21137-21144, https://doi.org/10.1021/acsomega.0c02837.
200. Chen, C.; Cai, W.; Long, M.; Zhou, B.; Wu, Y.; Wu, D.; Feng, Y. Synthesis of visible-light responsive graphene oxide/TiO2 composites with p/n heterojunction. *ACS Nano* **2010,** *4*, 6425-6432, https://doi.org/10.1021/nn102130m.

201. Tang, J.; Wang, J. Fe-based metal organic framework/graphene oxide composite as an efficient catalyst for Fenton-like degradation of methyl orange. *RSC Adv.* **2017,** *7*, 50829-50837, https://doi.org/10.1039/C7RA10145G.
202. Li, L.; Zhang, J.; Fu, X.; Xiao, P.; Zhang, M.; Liu, M. One-pot solid-state reaction approach to synthesize Ag-Cu2O/GO ternary nanocomposites with enhanced visible-light-responsive photocatalytic activity. *Int. J. Photoenergy* **2017,** *2017*, https://doi.org/10.1155/2017/8983717.
203. Zhang, L.; Wu, K.; Zhou, Y.; Guo, J.; Wu, H.; Yu, F.; Wu, Y. Synthesis of MnO 2@ graphene oxide flower-like nanocomposite as adsorbent for methyl orange decolouration. *Micro Nano lett.* **2017,** *12*, 335-337, https://doi.org/10.1049/mnl.2016.0615.
204. Raliya, R.; Avery, C.; Chakrabarti, S.; Biswas, P. Photocatalytic degradation of methyl orange dye by pristine titanium dioxide, zinc oxide, and graphene oxide nanostructures and their composites under visible light irradiation. *Appl. Nanosci.* **2017,** *7*, 253-259, https://doi.org/10.1007/s13204-017-0565-z.
205. Mangadlao, J. D.; Cao, P.; Choi, D.; Advincula, R. C. Photoreduction of graphene oxide and photochemical synthesis of graphene–metal nanoparticle hybrids by ketyl radicals. *ACS Appl. Mater. Interfaces* **2017,** *9*, 24887-24898, https://doi.org/10.1021/acsami.7b06275.
206. Yan, Q.; Xie, X.; Lin, C.; Zhao, Y.; Wang, S.; Liu, Y. Synthesis of graphene oxide/Ag 3 PO 4 composite with enhanced visible-light photocatalytic activity. *J. Mater. Sci.: Mater. Electron.* **2017,** *28*, 16696-16703, https://doi.org/10.1007/s10854-017-7582-2.
207. Liu, R.; Li, X.; Li, S.; Zhou, G. Three-dimensional titanate–Graphene oxide composite gel with enhanced photocatalytic activity synthesized from nanofiber networks. *Catal. Today* **2017,** *297*, 264-275, https://doi.org/10.1016/j.cattod.2016.12.046.
208. Chao, D.; Liu, Y.; Zhu, Z. Facile fabrication of magnetically separable Ag3PO4/CoFe2O4/GO composites with enhanced visible light photocatalytic performance. *Mater. Lett.* **2018,** *217*, 239-242, https://doi.org/10.1016/j.matlet.2018.01.084.
209. Feng, Q.; Li, S.; Ma, W.; Fan, H.-J.; Wan, X.; Lei, Y.; Chen, Z.; Yang, J.; Qin, B. Synthesis and characterization of Fe3O4/ZnO-GO nanocomposites with improved photocatalytic degradation methyl orange under visible light irradiation. *J. Alloys Comp.* **2018,** *737*, 197-206, https://doi.org/10.1016/j.jallcom.2017.12.070.
210. Tran, D. T.; Nguyen, M. T.; Le, T. T. T.; Ha, M. N.; Nguyen, M. V.; Pham, T. D. Enhanced photocatalytic degradation of methyl orange using ZnO/graphene oxide nanocomposites. *Res. Chem. Intermed.* **2018,** *44*, 3081-3095, https://doi.org/10.1007/s11164-018-3294-3.
211. Wu, Z.; Wang, L. Graphene oxide (GO) doped CeO2 as potential enhancer of methyl orange degradation. *Fuller. Nanotub. Car. N.* **2019,** *27*, 344-350, https://doi.org/10.1080/1536383X.2019.1573818.
212. Abbasi, S.; Ahmadpoor, F.; Imani, M.; Ekrami-Kakhki, M.-S. Synthesis of magnetic Fe3O4@ ZnO@ graphene oxide nanocomposite for photodegradation of organic dye pollutant. *Int. J. Environ. Anal. Chem.* **2020,** *100*, 225-240, https://doi.org/10.1080/03067319.2019.1636038.
213. Zhang, X.; Wei, W.; Zhang, S.; Wen, B.; Su, Z. Advanced 3D nanohybrid foam based on graphene oxide: Facile fabrication strategy, interfacial synergetic mechanism, and excellent photocatalytic performance. *Sci. China Mater.* **2019,** *62*, 1888-1897, https://doi.org/10.1007/s40843-019-9473-2.
214. Govindan, K.; Suresh, A.; Sakthivel, T.; Murugesan, K.; Mohan, R.; Gunasekaran, V.; Jang, A. Effect of peroxomonosulfate, peroxodisulfate and hydrogen peroxide on graphene oxide photocatalytic performances in methyl orange dye degradation. *Chemosphere* **2019,** *237*, 124479, https://doi.org/10.1016/j.chemosphere.2019.124479.
215. Wang, Q.; Li, Y.; Huang, L.; Zhang, F.; Wang, H.; Wang, C.; Zhang, Y.; Xie, M.; Li, H. Enhanced photocatalytic degradation and antibacterial performance by GO/CN/BiOI composites under LED light. *Appl. Surf. Sci.* **2019,** *497*, 143753, https://doi.org/10.1016/j.apsusc.2019.143753.
216. Nguyen, T. H.; Vu, A. T.; Wu, J. C.-S.; Le, M. T. Photocatalytic Degradation of Phenol and Methyl Orange with Titania-Based Photocatalysts Synthesized by Various Methods in Comparison with ZnO–Graphene Oxide Composite. *Top. Catal.* **2020,** *63*, 1215-1226, https://doi.org/10.1007/s11244-020-01361-5.
217. Ashraf, M. A.; Yang, Y.; Fakhri, A. Synthesis of NiS–MoO3 nanocomposites and decorated on graphene oxides for heterogeneous photocatalysis, antibacterial and antioxidant activities. *Ceramics Int.* **2020,** *46*, 8379-8384, https://doi.org/10.1016/j.ceramint.2019.12.070.
218. Zhang, Z.; Sun, L.; Wu, Z.; Liu, Y.; Li, S. Facile hydrothermal synthesis of CuO–Cu 2 O/GO nanocomposites for the photocatalytic degradation of organic dye and tetracycline pollutants. *New J. Chem.* **2020,** *44*, 6420-6427, https://doi.org/10.1039/D0NJ00577K.

219. Das, T. R.; Sharma, P. K. Bimetal oxide decorated graphene oxide (Gd2O3/Bi2O3@ GO) nanocomposite as an excellent adsorbent in the removal of methyl orange dye. *Mater. Sci. Semicond. Process.* **2020,** *105*, 104721, https://doi.org/10.1016/j.mssp.2019.104721.
220. Djouani, R.; Kamali, A. R. Preparation of photoactive graphene oxide-Cu2O/Cu nanostructures by the electrochemical treatment of CuNi leaching solutions using graphite electrodes. *Diam. Relat. Mater.* **2020,** *109*, 108088, https://doi.org/10.1016/j.diamond.2020.108088.
221. Jamila, G. S.; Sajjad, S.; Leghari, S. A. K.; Long, M. Nitrogen doped carbon quantum dots and GO modified WO3 nanosheets combination as an effective visible photo catalyst. *J. Hazard. Mater.* **2020,** *382*, 121087, https://doi.org/10.1016/j.jhazmat.2019.121087.
222. Lin, C.; Gao, Y.; Zhang, J.; Xue, D.; Fang, H.; Tian, J.; Zhou, C.; Zhang, C.; Li, Y.; Li, H. GO/TiO 2 Composites as a highly active photocatalyst for the Degradation of Methyl Orange. *J. Mater. Res.* **2020,** *35*, 1307-1315, https://doi.org/10.1557/jmr.2020.41.
223. Noor, S.; Sajjad, S.; Leghari, S. A. K.; Flox, C.; Kallio, T. Efficient electrochemical hydrogen evolution reaction and solar activity via bi-functional GO/CO3O4–TiO2 nano hybrid structure. *Int. J. Hydrog. Energy* **2020,** *45*, 17410-17421, https://doi.org/10.1016/j.ijhydene.2020.04.240.
224. Purkayastha, M. D.; Sil, S.; Singh, N.; Ray, P. P.; Darbha, G. K.; Bhattacharyya, S.; Mallick, A. I.; Majumder, T. P. Sonochemical synthesis of nanospherical TiO2 within graphene oxide nanosheets and its application as a photocatalyst and a Schottky diode. *FlatChem* **2020,** *22*, 100180, https://doi.org/10.1016/j.flatc.2020.100180.
225. Xie, X.; Wang, S.; Zhang, Y.; Ding, J.; Liu, Y.; Yan, Q.; Lu, S.; Li, B.; Liu, Y.; Cai, Q. Facile construction for new core-shell Z-scheme photocatalyst GO/AgI/Bi2O3 with enhanced visible-light photocatalytic activity. *J. Colloid Interface Sci.* **2021,** *581*, 148-158, https://doi.org/10.1016/j.jcis.2020.07.128.
226. Mandal, P.; Saha, M. Photodegradation Behaviour of Nitrogen-Containing Graphene Derivatives Towards Pollutant Dyes and Real-Time Assessment on Aquatic Weed. *Biointerface Res. Appl. Chem.* **2022**, *12*, 4357-4373, https://doi.org/10.33263/BRIAC124.43574373.
227. Mandal, P.; Nath, K. K.; Saha, M. Efficient Blue Luminescent Graphene Quantum Dots and their Photocatalytic Ability Under Visible Light. *Biointerface Res. Appl. Chem*. **2021**, *11*, 1059-1064, https://doi.org/10.33263/BRIAC111.81718178.